

Design and Stereoselective Synthesis of Retinoids with Ferrocene or *N*-Butylcarbazole Pharmacophores that Induce Post-Differentiation Apoptosis in Acute Promyelocytic Leukemia Cells

Diana Ivanova,^[a, b] Hinrich Gronemeyer,^{*[b]} and Angel R. de Lera^{*[a]}

New ferrocene and *N*-alkylcarbazole retinoids were designed and synthesized stereoselectively in good yields. A number of these synthesized ligands, in particular **2**, **3**, and **11**, were found to exhibit a high RAR α activation potential and to effectively induce post-differentiation apoptosis in NB4 acute promyelocytic leukemia (APL) cells. Increasing the length of the side chain attached to the heterocycle of the carbazole retinoids creates new opportunities for altered compound catabolism and for fine-tuning of the apoptosis-inducing potential of the ligand. In the carbazole series of new retinoids, maximal

activity was established for *N*-butylcarbazole analogue **11** in all assays (i.e., RAR α activation, differentiation induction, and apoptosis induction). Study of the mechanism of apoptosis revealed an activation of initiator caspases-8 and -9, followed by efficient cleavage of effector caspase-3 on day 6 of treatment. Subsequent induction of a caspase cascade in NB4 cells triggered ultimate leukemic cell death. The selected ligands **2**, **3**, and **11** may provide alternate options for the treatment of APL in cases of life-threatening ATRA syndrome, resistance, and high toxicity to conventionally used retinoids.

Introduction

Leukemia is a hematological disease characterized by an abnormal proliferation of immature white blood cells. The excessive number of leukocytes leads also to an imbalance in the count of other blood cells such as platelets and erythrocytes. In acute promyelocytic leukemia (APL), the proliferating cells are promyelocytes whose differentiation into granulocytes is blocked. According to the French–American–British classification system, APL is the M3 subtype of acute myelogenous leukemia (AML); this subtype represents 5–8% of all AML cases.

In 95–98% of cases, APL is caused by a balanced reciprocal chromosomal translocation t(15;17)(q22;q12–21) that fuses the retinoic acid receptor alpha gene (RAR α), located on chromosome 17, with the promyelocytic leukemia gene (PML), initially located on chromosome 15.^[1] RAR α , β , and γ are ligand-dependent transcription factors that regulate gene expression by direct binding to DNA. Like other nuclear receptors, RARs have a modular structure with six domains (A–F), which include the DNA binding domain (C) and the ligand binding domain (E). Oncogenic properties are attributed only to the PML–RAR α (domains B–F) fusion protein. The reciprocal fusion protein RAR α –(domain A)–PML can be found in 80% of APL cases, but no oncogenic functions can be associated with it.^[2] According to the ‘two-hit’ model, fusion proteins induce a ‘pre-leukemic’ state, while secondary genetic lesions that favor the survival of genetically modified cells lead to leukemogenesis.^[3]

In rare cases of APL, other genes are fused to the RAR α gene such as promyelocytic leukemia zinc finger (PLZF), nucleophosmin (NPM), nuclear mitotic apparatus protein (NuMA), or signal transducer and activator of transcription 5b (STAT5b) genes. The fusion oncoproteins cause both ‘loss of normal

functions’ as well as ‘gain of new oncogenic functions’ of the fusion partners. Oncoproteins form multiprotein co-repressor complexes with histone deacetylases (HDACs), methyl-CpG binding proteins, and DNA methyltransferases that cause transcriptional repression of adjacent genes.

Patients with PML–RAR α , NPM–RAR α , and NuMA–RAR α are sensitive to all-*trans*-retinoic acid (ATRA), which in combination with anthracycline antibiotics and consolidation therapy leads to remission of up to 80–90% of APL patients. The problem is that about one quarter of the newly diagnosed patients relapse, become resistant to ATRA, and should be subjected to bone marrow transplantation and treatment with highly toxic arsenic trioxide. Patients with PLZF–RAR α or STAT5b–RAR α are not sensitive to ATRA due to stronger affinity of the co-repressors that bind not only to the RAR α part but also to its partner part in the fusion protein.^[4]

[a] Dr. D. Ivanova,[†] Prof. A. R. de Lera
Department of Organic Chemistry, University of Vigo, 36310 Vigo (Spain)
Fax: (+34) 986-812-316
E-mail: qolera@uvigo.es

[b] Dr. D. Ivanova,[†] Prof. H. Gronemeyer
Institute of Genetics and Molecular and Cellular Biology
BP 10142, Strasbourg, 67404 Illkirch Cedex (France)
Fax: (+33) 388-653-437
E-mail: hg@igbmc.fr

[†] Present address: ChimOrbel Ltd.
83 Blvd. Nicola Petkov, 1614 Sofia (Bulgaria)

Supporting information for this article is available on the WWW under <http://dx.doi.org/10.1002/cmdc.201100065>: characterization data for various intermediate compounds in the synthesis of ligands 1–14.

The therapy of APL with ATRA or RAR α agonists is based on their binding with RAR α and the induction of a major allosteric change in the protein.^[5] This conformational effect leads to dissociation of the co-repressors and association of co-activators (with histone acetyltransferase activity) with the receptor. Binding of co-repressors and co-activators to the receptor is mutually excluded. Histone acetylation leads to an open chromatin conformation at the promoter site of the genes that regulate the differentiation process. Then, general transcription factors (TFIIB, TFIID, etc.), Mediator, and RNA polymerase II are recruited, and the transcription is started. Thus, ATRA or RAR α agonists reverse the balance in NB4 APL cells from the oncogenic PML–RAR α to the normal RAR α . In cancer cells, these processes occur at pharmacological concentrations of ATRA ($\sim 10^{-8}$ – 10^{-6} M) that are higher than its normal physiological concentration ($\sim 10^{-9}$ M).

ATRA is the natural ligand of RARs, whereas 9-*cis*-retinoic acid is a pan-agonist that activates both RARs and retinoid X receptors (RXRs).^[6] ATRA-like compounds are excluded by the sharper bend in the RXR ligand binding pocket (RXR-LBP), which accommodates conformationally flexible analogues of 9-*cis*-RA. RXR agonists (retinoids) activate RXR in *permissive* heterodimers (such as PPAR α –RXR, PPAR γ –RXR, and LXR–RXR) that can also be activated by ligands of the RXR partner protein. *Non-permissive* heterodimers (such as RAR–RXR, TR–RXR, and VDR–RXR)^[7] are activated only by ligands of the RXR partner protein; however, retinoids can act in synergy with them. RXR agonists can cause undesirable therapeutic side effects such as an increase in the level of triglycerides (by LXR–RXR), an imbalance in glucose metabolism (by PPAR γ –RXR), or a decrease in thyroid hormone levels (by TR–RXR).^[8] In contrast, RAR class-selective agonists act preferably through RAR pathways and therefore do not result in therapeutic side effects caused by activation of RXR pathways.

Herein we report the stereoselective synthesis of a series of ferrocene, phenanthrene, and *N*-alkylcarbazole retinoids **1–14**. New RAR class-selective (i.e., RAR versus RXR) agonists (compounds **2**, **3**, and **8–13**) were identified, and their potential to induce post-differentiation apoptosis in NB4 APL cells was established.^[9] Details of the caspase cascade that triggered apoptosis in APL cells after treatment with the new potential drugs were also investigated.

Ferrocene derivatives **2** and **3** are the first organometallic compounds determined to be RAR class-selective agonists. An alkyl side chain at the nitrogen atom of the carbazole retinoids (polyaromatic retinoid) **8–13** was envisaged to possibly alter the catabolism, pharmacokinetics, and pharmacodynamics of the ligand in order to decrease its toxicity and to improve its therapeutic index and efficacy.

N-alkylcarbazole derivatives have been studied as electrophotographic photoreceptors.^[10] A very interesting and atypical retinoid, AGN 193198 (Allergan Inc., Irvine, CA, USA), which is structurally related to **11**, was extremely effective in the induction of apoptosis in cancer cells (prostate, breast, and gastrointestinal carcinoma cells) by caspase (-3, -8, -9, and -10) cleavage, but neither RAR/RXR activation nor cell differentiation were registered.^[11]

Ferrocenyl compounds have been analyzed as chromophores with potential technical applications.^[12,13] The ethyl ester of ferrocenyl retinoic acid has been studied with regard to papilloma regression in mouse models.^[14] Ferrocene analogues of the breast cancer drug tamoxifen and its active metabolite hydroxytamoxifen, analogously termed ferrocifens, have been synthesized and showed antiproliferative properties in both hormone-dependent and hormone-independent breast cancer cells.^[15] Therefore, ferrocene compounds revealed new perspectives in pharmacology and particularly in oncology.^[16]

The compounds with strongest anticancer activity, i.e., **2** and **3** from the ferrocene series and **11** from the *N*-alkylcarbazole series that were identified here as new apoptogenic molecules in NB4 APL cells, have potential application in cases of either increased catabolism, resistance to conventionally used retinoid drugs, or retinoic acid syndrome, of which the latter represents a life-threatening complication in APL patients that requires holding ATRA for a period of time.

Results and Discussion

The new anticancer retinoids are the result of several series of experiments: 1) rational design and stereoselective synthesis of RAR class-selective retinoids with ferrocene-, phenanthrene-, or *N*-alkylcarbazole-containing pharmacophores; 2) analysis of the RAR/RXR selectivity of the ligands; 3) correlation of the RAR α activation potential with the induction of post-differentiation apoptosis in NB4 cells, according to the mechanism of APL; and 4) identification of molecular targets of the ligands in extrinsic and intrinsic apoptotic pathways.

RAR α activation is the target process in the induction of post-differentiation apoptosis in NB4 cells harboring PML–RAR α fusion protein. RAR β is a known tumor suppressor induced by retinoids, whereas RAR γ is not involved in the differentiation of NB4 cells.

Design and synthesis of new RAR class-selective agonists

New ferrocene-, phenanthrene-, and carbazole-containing pharmacophores were designed to contain hydrophobic cyclic groups and all-*trans* side chains in order to bind to the L-shaped RAR ligand binding domain (LBD) and to be discriminated by the L-shaped RXR ligand binding pocket (LBP). A terminal carboxylic group in the structures of all studied retinoids guaranteed successful anchoring of the ligand in the LBP of the corresponding retinoic acid receptor.

Our previous study on the synthesis and biological activity of phenanthrene retinoids revealed that the phenanthrene group can be accommodated in the LBPs of RAR α and RAR β .^[17] These results prompted us to synthesize other phenanthrene retinoids in order to study their differential RAR/RXR activation potential and to identify new selective retinoid agonists in the phenanthrene group of retinoids. The promising results obtained in the investigations of ferrocene analogues of anticancer compounds *in vitro* were the rational background to generate ferrocene retinoic acid analogues that may

be able to induce post-differentiation apoptosis in NB4 APL cells.

Retinoids **1–14** with all-*trans* side chains were designed by replacement of the natural β -ionone ring of ATRA with ferrocene, phenanthrene, or alkylated carbazole groups. These modifications provided an opportunity to study experimentally the adaptation of both the ligand and the hydrophobic LBP to trigger transactivation of the receptor. Ligand docking is envisaged in the future based on the recent determination of the crystal structure of RAR α ^[18]—the target receptor for induction of post-differentiation apoptosis in NB4 cells according to the accepted mechanism of APL. While this work started, only the structures of ligand binding domains of RAR β ,^[19] RAR γ ,^[20] and an antagonist-bound RAR α ^[21] as a heterodimer with RXR had been resolved by X-ray crystallography.

Modifications of the side chain (in length and volume) were made in order to study empirically the restrictions and the flexibility of all RAR LBPs. For example, a phenyl group was introduced at different position of the side chain in compounds **1**, **4**, **5**, and **7**. Compounds **3** and **8** were modified to contain two or one isoprene units in the side chain, respectively. In retinoids **2**, **6**, and **9–14**, the presence of a terminal benzoic acid group in a *trans*-configured side chain was envisaged to elicit pan-RAR activation analogously to TTNPB [*p*-[(*E*)-2-(5,6,7,8-tetrahydro-5,5,8,8-tetramethyl-2-naphthyl)propen-1-yl]benzoic acid]—a pan-RAR agonist, the predecessor of the family of synthetic arotinoids (retinobenzoic acids).

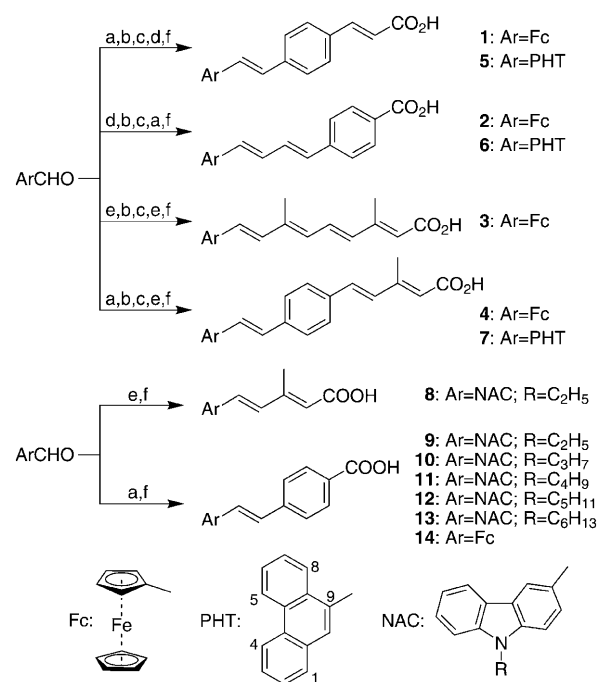
An alkyl side chain of increasing length, attached to the heterocycle of the carbazole arotinoids, was foreseen to fine-tune the potentials with regard to RAR α activation and induction of post-differentiation apoptosis of the new analogues **8–13**. The molecular basis for the maximal RAR α -agonist activity of compound **11** from the carbazole group of arotinoids will be elucidated in the future by ligand docking in an agonist-bound RAR α LBD.

In addition, the alkylated backbone of the heterocycle was foreseen to create an opportunity for an altered catabolism and decreased toxicity of the ligand (pharmacologically oriented drug design). It was taken into consideration that heteroarotinoids have been found to be less toxic^[22] than TTNPB because of the metabolic stability of its tetramethylated cyclohexenyl ring.

Stereoselective synthesis of the ligands

Horner–Wadsworth–Emmons (HWE) olefination was selected as a key reaction for the synthesis of new *N*-alkylcarbazole, ferrocene, and phenanthrene retinoid ligands because of the high yields and stereoselectivity in the reactions of suitably constructed C₂-, C₅-, or benzyl phosphonates with corresponding aromatic aldehydes (Scheme 1). Environmentally hazardous metals such as lead and palladium were not used in the synthesis of our compounds, considering their potential application in the pharmaceutical industry.

All-*trans* configurations of the compounds were maintained along the reaction sequences. Only *trans* isomers were obtained in the HWE reactions of the corresponding aromatic al-



Scheme 1. Synthesis of ferrocene, phenanthrene, and *N*-alkylcarbazole retinoids **1–14**.^[24] a) (EtO)₂P(O)CH₂C₆H₄CO₂Me, *n*BuLi, DMPU, THF, –70 °C, 30 min, then –40 °C, 2 h; b) DIBAL-H, THF, –70 °C, 1–2 h; c) MnO₂, CH₂Cl₂, RT, 2–6 h; d) (EtO)₂P(O)CH₂CO₂Et, *n*BuLi, DMPU, THF, –70 °C, 30 min, then –40 °C, 2 h; e) (EtO)₂P(O)CH₂C(CH₃)=CHCO₂Et, *n*BuLi, DMPU, THF, –70 °C, 30 min, then –40 °C, 2 h; f) MeOH/5 N NaOH, reflux, 2–14 h; 6 N HCl. See Experimental Section for reaction times of various analogues for steps c) and f).

dehydes with C₂- or benzyl phosphonoesters. This result was expected because the reaction mechanism involves the formation of a phosphonoester carbanion intermediate that is stabilized by delocalization of the negative charge. The nucleophilic attack of the carbanion on the carbon atom of the aldehyde group proceeds under thermodynamic control, thus leading to stereoselective synthesis of the thermodynamically more stable product with *trans* configuration at the newly formed double bond. Minor *2E/2Z* isomerization (~10%) was registered by NMR analysis of the reaction mixture only in the HWE reactions with C₅-phosphonate. This effect was due to the low energy barrier to isomerization of the terminal double bond and did not depend on the initial *2E/2Z* ratio in the C₅-phosphonate.^[23] In the final step, the purified all-*trans* isomer of the ester from the HWE reaction was held at reflux in methanolic sodium hydroxide to obtain the desired acid in high yields (Table 1, column f). The new potential anticancer agents were characterized by NMR, IR, HRMS, and/or elemental analysis (see Experimental Section below).

Differential RAR/RXR transactivation by the new retinoids

Identification of new transcriptionally competent ligands for nuclear receptors was carried out using the 'domain-swap' method, which is based on transcription of the protein-coding genes of interest followed by ligand-induced receptor activation in genetically engineered 'reporter' cells (baculovirus-in-

Table 1. Yields of compounds in the multistep synthesis of retinoids 1–14.

Compd	Group ^[a]	a ^[b]	b ^[b]	c ^[b]	d ^[b]	e ^[b,c]	f ^[b]
1	Fc	51	100	63	96	–	77
2	Fc	68	100	83	96	–	100
3	Fc	–	100	67	–	100	100
4	Fc	51	100	63	–	82	94
5	PHT	75	73	98	71	–	99
6	PHT	100	100	92	80	–	83
7	PHT	75	73	98	–	75	100
8	NAC	–	–	–	–	90	90
9	NAC	100	–	–	–	–	94
10	NAC	74	–	–	–	–	99
11	NAC	75	–	–	–	–	100
12	NAC	57	–	–	–	–	100
13	NAC	76	–	–	–	–	100
14	Fc	51	–	–	–	–	99

[a] Fc = ferrocene, PHT = phenanthrene, NAC = *N*-alkylcarbazole. [b] Stages of the synthesis according to Scheme 1. [c] *2E/2Z* ratio is ~90:10 (see text for details).

fectured insect cells, CV-1 cells, human HeLa cells, etc.).^[25] This was the method of choice for identification of new RAR α agonists instead of computer-aided ligand docking considering the fact that no crystal structure of an agonist-bound RAR α LBD is at present available. In our experiments, HeLa cells were transfected with two types of recombinant DNA: 1) a chimeric gene that generates a fusion protein DBD(Gal4)–LBD(RAR) consisting of the DNA binding domain (DBD) of Gal4 (a yeast transcription factor) fused to the ligand binding domain (LBD) of the nuclear receptor of interest; and 2) a second expression vector, (17m)₅– β G-*luc*, that contains a luciferase (*luc*) reporter gene under the control of five copies of the cognate GAL4 response element [(17m)₅] in front of a β -globin promoter.^[26] Activation of RAR LBD by an agonist in the presence of luciferase [EC 1.13.12.7], coenzyme A, and luciferin generates luminescence, which can be detected using a luminometer.

This method is insensitive to endogenous retinoic acid receptors because they cannot recognize the Gal4 response elements. A mutant of RXR β (RXR β Δ AB) was used to eliminate false-positive signals.^[27] RXR β transactivation was used to evaluate the transactivation at all three RXRs (α , β , and γ) because of the similar structure of the corresponding RXR LBDs.

Structure–activity relationship of ligand-induced RAR transactivation

All-*trans*-retinoids **2**, **3**, and **8–13** were found to be RAR class-selective ligands (Table 2). All compounds studied here were discriminated by the L-shaped RXR LBD because of the flexure limit of all-*trans* side chains.

Ferrocenyl derivatives **1** and **4** with a phenyl group in the central region of the side chain activated RAR β and RAR γ . The prevention of RAR α transactivation due to steric hindrance, which is imposed by the presence of a phenyl group with two adjacent double bonds in the middle region of the polyenic side chain, was empirically established here. Ligand docking in

Table 2. Differential RAR/RXR activation by new RAR class-selective retinoids.

Compd	Group	RAR α	RAR β	RAR γ	RXR β	Selectivity ^[a]
vehicle	ctrl	1.00	1.00	1.00	1.00	vehicle ctrl
ATRA	ctrl	17.62	9.61	4.17	ND ^[b]	RAR
9- <i>cis</i> -RA	ctrl	ND	ND	ND	30.03	pan-RAR/RXR
TTNPB	ctrl	46.06	25.03	6.40	ND	RAR
BMS 753 ^[c]	ctrl	45.49	ND	ND	ND	RAR α agonist
BMS 641 ^[c]	ctrl	ND	17.52	ND	ND	RAR β agonist
BMS 961 ^[c]	ctrl	ND	ND	6.50	ND	RAR γ agonist
1	Fc	1.26	12.66	6.17	1.69	RAR β,γ
2	Fc	20.78	19.60	10.22	2.05	RAR
3	Fc	13.51	9.33	5.28	2.58	RAR
4	Fc	3.28	11.92	9.65	1.77	RAR β,γ ; weak RAR α
6	PHT	2.48	4.62	1.32	1.35	partial RAR β
8	NAC	13.37	20.56	6.85	1.70	RAR
9	NAC	20.60	19.89	8.81	2.17	RAR
10	NAC	26.68	19.94	9.73	2.39	RAR
11	NAC	31.36	19.55	9.18	2.21	RAR
12	NAC	21.46	19.30	10.74	2.17	RAR
13	NAC	13.66	18.87	9.26	1.88	RAR

[a] RAR/RXR activation is presented as fold induction, defined as the ratio of the relative luciferase units (RLU) detected in the presence of the corresponding ligand (at 10⁻⁶ M) over the RLU of the vehicle control in HeLa cells. Fold induction of 2.0–3.0 was considered very low activation, a value of 3.0–3.5 as weak activation, and a value >3.5 as considerable activation. All values are compared with the data of the corresponding positive control. The values represent the average of four measurements from two separate experiments with duplicate determinations. [b] ND: not detected. [c] Selective agonists BMS 753, BMS 641, and BMS 961 were kindly provided by Bristol-Myers Squibb.

the RAR α LBD may reveal the structural basis for the maximal RAR α activation elicited by the *N*-butyl derivative **11** from the RAR class-selective carbazole series **8–13**.

We found previously that a phenanthrene group in the hydrophobic moiety of the molecule, as in compound **6**, creates steric hindrance with RAR γ Met272.^[17] Retinoid **6** is discriminated also by RAR α because of the presence of a phenyl ring with two double bonds in the central part of the side chain, as discussed above. Being discriminated by RAR α , RAR γ , and RXR, retinoid **6** is partial RAR β agonist because maximal RAR β activation could not be reached by an increase in ligand concentration. The binding of long molecules such as **5** and **7** and short molecules such as **14** was abolished by the length restrictions for successful anchoring of the ligand in all RAR LBDs.

The new RAR class-selective compounds were obtained to broaden the spectrum of potentially less toxic drugs in APL therapy. The RAR class selectivity of the new ligands **2**, **3**, and **8–13** is promising for further preclinical trials, as these compounds may avoid undesirable side effects (imbalance in triglyceride, glucose, and thyroid hormone levels) due to RXR-permissive heterodimer activation. Therefore, we examined whether the high RAR α activation potential of these compounds correlates with the induction of post-differentiation apoptosis in NB4 cells according to the mechanism of APL. Using fluorescence-activated cell sorting (FACS) analysis, we selected compounds **2** and **3** from the ferrocene series and *N*-butyl derivative **11** from the carbazole series as strongest

apoptogenic substances in the corresponding groups of ligands.

Correlation of RAR α activation with differentiation and apoptosis induction in NB4 cells by new anticancer agents

NB4 cells undergo differentiation in response to treatment with ATRA or RAR α agonists at pharmacological concentrations. In the ferrocene series, only ligands **2** and **3** (at 10^{-6} M), which have a high RAR α activation potential, demonstrated high differentiation- and apoptosis-inducing activities, according to the mechanism of APL. Arotinoid **11** triggered maximal post-differentiation apoptosis in NB4 cells because of its maximal potential in the carbazole series of ligands to activate RAR α .

As detected by FACS analysis, NB4 cells differentiated into granulocytes and expressed CD11c glycoproteins on their surface in response to treatment with new RAR class-selective retinoids **2**, **3**, and **8–13** at 10^{-6} M concentration (Figure 1A). Maturation of NB4 cells into monocytes and cell-surface expression of CD14 was not induced (data not shown).

Retinoid-induced apoptosis of leukemic cells (HL60, NB4, etc.) is a post-differentiation process.^[28] Retinoids that triggered maturation in a high percentage of NB4 cells but at low intensity of the labeling were possibly not apoptogenic because terminal differentiation of the leukemic cells has not been reached. Apoptosis was examined by FACS analysis using double labeling of treated NB4 cells with Annexin V-FITC and

propidium iodide (PI) to discriminate necrotic from apoptotic cells. Ferrocene ligands **2** and **3** and *N*-butylcarbazole arotinoid **11** with high RAR α activation potential and consequently high differentiation-inducing potential from the corresponding series of new pharmacophores triggered effectively apoptosis in NB4 cells (Figure 1).

Both ferrocene ligands **2** and **3** have a high potential to induce efficiently post-differentiation apoptosis in NB4 APL cells. As the ethyl ester of ferrocene retinoic acid **3** was formerly investigated in a papilloma regression study,^[14] we selected the new compound **2** as a representative RAR agonist from the ferrocene series of retinoids for analysis of its mechanism of activity. Thus, highly efficient retinoid **2** from the ferrocene series and the most active compound **11** from the *N*-alkylcarbazole series were selected for Western blot analysis to examine their mechanism of apoptosis induction.

Western blot analysis pertaining to apoptosis induction

Induction of tumor necrosis factor-related apoptosis-inducing ligand (TRAIL) by the extrinsic apoptosis pathway was the first cellular target, detected on day 3 after treatment of NB4 cells with ferrocene retinoid **2** (Figure 2A). Weak TRAIL expression was registered at treatment of NB4 cells with *N*-butylcarbazole arotinoid **11** (Figure 2B). Constitutive expression of at least one TRAIL receptor (DR5) in NB4 cells was demonstrated by Western blotting.

TRAIL triggered formation of the death-inducing signaling complex (DISC) that effectively induced subsequently the activation of initiator caspase-8 by cleavage, followed by cleavage of effector caspase-3. Western blot analysis proved activation of caspase-8 by formation of p18 and p43/41 fragments that induced efficient cleavage of caspase-3 to fragment p17. Minor detection of fragment p17 from caspase-3 in the vehicle control was due to spontaneous death of minimal amounts of NB4 cells from the non-treated cells. Simultaneous action of caspases-3, -8, and -9 accelerated apoptosis and led to massive leukemic cell death on the day 6 of treatment.

Expression of the BH3-interacting domain death agonist (Bid), a protein that connects the intrinsic and extrinsic apoptosis pathways, was not induced. Nevertheless, upregulation and cleavage of initiator caspase-9 by the intrinsic apoptosis pathway was triggered at the same time as caspase-8 by the extrinsic apoptosis pathway. The *casp9* gene was detected to harbor a 2-bp-spaced direct repeat of a retinoic acid-responsive element (DR-2 RARE) in its second intron and was shown to be under the direct control of RAR in a previous study of carcinoma cells (MCF-7).^[29] This finding supports the direct activation of caspase-9 by retinoids.

An interesting protein with a molecular mass of ~25 kDa was detected by the antibody for caspase-9 at treatment with all studied synthetic or natural retinoids. This protein appeared on days 2–3 after beginning the treatment with retinoids even before TRAIL activation. The identification of this molecular target is of great interest to clarify the general mechanism underlying retinoid anticancer activity in APL in the future.

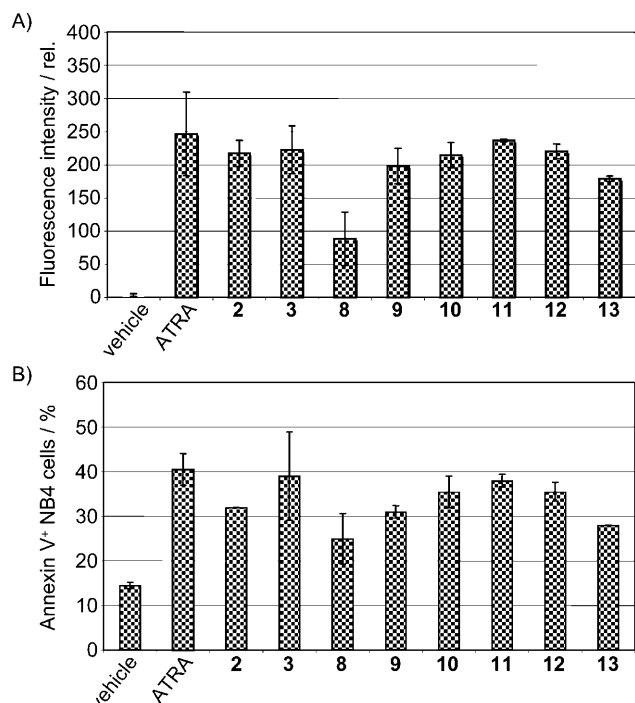


Figure 1. FACS analysis of A) differentiation induction (fluorescence intensity of CD11c⁺/PI⁻ cells) and B) apoptosis induction (percent Annexin V⁺ cells) in NB4 APL cells after six days of treatment with the new retinoid agonists **2**, **3**, and **8–13** (all at 1 μ M). Values represent the average \pm SD of two independent experiments.

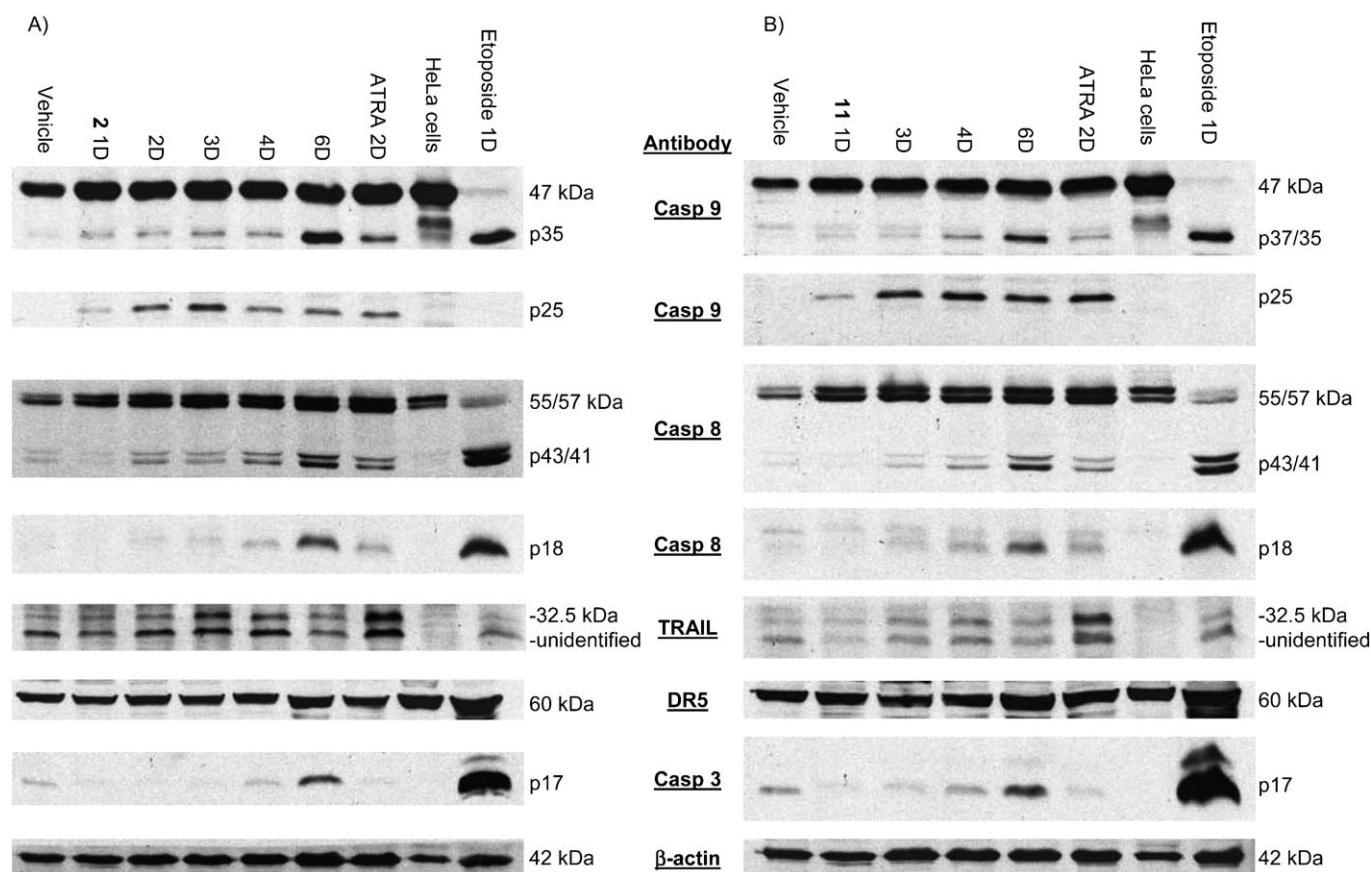


Figure 2. Western blot analysis of expression of caspase cascade proteins triggered by A) ferrocene retinoid **2** or B) *N*-butylcarbazole arotinoid **11**. Abbreviations 1D, 2D, ... denote day 1, day 2, ... of treatment. The total lysate of HeLa cells (cultured 2 days) was used as a positive control for DR5 expression, while the total lysate of NB4 cells treated with Etoposide (1 μ M) was used as a positive control for cleavage of caspases. The cells for vehicle control were maintained in culture during the treatment and showed identical immunoreactive proteins by Western blot for days 1, 3, and 6.

In summary, Western blot analysis to determine the mechanism of apoptosis revealed that the new ferrocene or *N*-butylcarbazole agonists with high RAR α activation potential induce post-differentiation apoptosis by early expression of TRAIL, which is followed by activation of initiator caspase-8 from DISC and activation of effector caspase-3. Beginning at the cell surface by the extrinsic pathway, cell death was accelerated by the intrinsic inducers of apoptosis. Activation of caspase-9, possibly under the direct control of RAR, amplified caspase-3 cleavage, and massive NB4 cell death occurred on day 6 of treatment.

Conclusions

We established an RAR class-selective (RAR versus RXR) agonist activity of the newly synthesized ferrocene retinoids **2** and **3** and *N*-butylcarbazole arotinoid **11**, all of which induce differentiation and apoptosis in NB4 cells. In accordance with the discussed mechanism of APL, post-differentiation apoptosis is a consequence of the high RAR α activation potential of the new pharmacophores.

The compounds were obtained stereoselectively in good yields by multistep chemical syntheses, using Horner–Wadsworth–Emmons olefination as a key reaction. All-*trans* configura-

tions of the double bonds were maintained along the reaction sequences.

An alkyl side chain with increasing number of carbon atoms was attached to the heterocycle of the carbazole arotinoids in order to fine-tune the ligand agonist activity. In the carbazole series of new pharmacophores a maximum of the activity was found for the *N*-butyl analogue **11** in all assays—RAR α activation, induction of differentiation, and induction of apoptosis in NB4 cells.

Western blot analysis of treated NB4 APL cells revealed that ferrocene retinoid **2** induced TRAIL expression and caspase-8 activation from the DISC by the extrinsic apoptosis pathway. TRAIL was detected on day 3 of treatment of NB4 cells with ferrocene retinoid **2**; however, it was weakly induced by the *N*-butylcarbazole arotinoid **11**. At least one TRAIL receptor (DR5) was constitutively expressed in NB4 APL cells.

At the same time, the intrinsic apoptosis pathway accelerated the retinoid-induced caspase cascade. Western blot analysis proved upregulation and cleavage of caspase-9, which is necessary for the assembly of the 'apoptosome'—the wheel-shaped heptameric death machine, consisting of caspase-9, cytochrome *c*, and Apaf-1 (apoptotic protease-activating factor 1).

BH3-interacting domain death agonist (Bid), a protein that connects the extrinsic and intrinsic apoptosis pathways, was not activated. This result was interpreted in terms of the finding that *casp9* was directly activated through the retinoic acid response element.^[29]

Coordinated action of caspases-3, -8, and -9 triggered a ligand-induced caspase cascade. FACS analysis of post-differentiation apoptosis and Western blot analysis proved massive death of NB4 cells on day 6 of treatment with ferrocene **2** or *N*-butylcarbazole ligand **11**.

The new apoptogenic ferrocene (**2** and **3**) and *N*-butylcarbazole (**11**) RAR agonists provide alternative options to study the treatment of APL in cases of life-threatening ATRA syndrome, high toxicity, or resistance to conventionally used retinoids in order to broaden the spectrum of available effective and less toxic drugs.

Perspectives

The RAR α activation by arotinoid **11** from the carbazole series of RAR agonists will be explained by ligand docking in an agonist-bound RAR α LBD.^[18]

Ferrocene retinoids **2** and **3** and *N*-butylcarbazole arotinoid **11**, which were evaluated as compounds with highest activity in our study, have promise for further preclinical studies of acute promyelocytic leukemia to determine their therapeutic index and efficacy. The *N*-butyl side chain of arotinoid **11** creates an opportunity for an altered catabolism of the compound and a decrease in drug toxicity compared with conventionally used retinoids.

Experimental Section

Chemistry

Materials and methods: Column chromatography (CC) was carried out on Kieselgel 60 (230–400 mesh, Merck), using EtOAc/hexane as eluent with an increasing percentage of EtOAc; thin-layer chromatography (TLC) was performed on silica gel-coated plates with fluorescence indicator (Merck), with visualization at 254 nm. NMR spectra were recorded on a Bruker-AMX400 instrument at 400.13 MHz (¹H NMR) or 100.61 MHz (¹³C NMR). Chemical shifts are given in δ [ppm], and coupling constants (*J*) are given in Hz. Assignments of resonances in ¹³C NMR spectra, which were supported by DEPT135 spectra, are: CH₃(q), CH₂(t), CH(d), C(s). IR spectra were registered on a JASCO FTIR-4200 spectrometer; peaks are given in $\tilde{\nu}$ [cm⁻¹] with intensities s (strong), m (medium), or w (weak). MS (EI, 70 eV) spectra were recorded on a VG-Autospec M apparatus. Melting points (mp) were determined on a Stuart Scientific apparatus.

Carbazole, triethyl phosphonoacetate, ferrocene aldehyde, and phenanthrene-9-carbaldehyde were purchased from Sigma-Aldrich. Other phosphonates were obtained by standard procedures: triethyl 3-methyl-4-phosphono-2-butenate (C₅-phosphonate) was synthesized by bromination of the methyl ester of 3,3'-dimethylacrylic acid with an equimolar amount of *N*-bromosuccinimide in the presence of traces of dibenzoyl peroxide in CCl₄ (reflux, 6 h), followed by an Arbuzov reaction of the resulting bromomethyl derivative with a slight excess (1.1-fold) of P(OEt)₃ (reflux, 4 h). *p*-[(Diethylphosphono)methyl]benzoate (aromatic phosphonate) was ob-

tained in an analogous procedure from the methyl ester of *p*-toluic acid.

General procedures: All manipulations with isomerizable products were performed under low light in amber glassware. The synthesized retinoids were stored for five years at –80 °C in the dark; all biological assays were performed with compounds from deep frozen (–80 °C) storage. HWE reactions and reductions with DIBAL-H were carried out in flame-dried flasks.

Horner–Wadsworth–Emmons (HWE) reactions: To a stirred solution of the corresponding phosphonate (1.75 mmol) and DMPU^[30] (3.45 mmol) in dry THF (4 mL) was added *n*BuLi (1.75 mmol) at 0 °C under argon atmosphere. This temperature was maintained for 30 min. After that, the temperature was decreased to about –70 °C, and a solution of the corresponding aldehyde (1.17 mmol) in THF (2 mL) was added dropwise. The reaction mixture was stirred for 30 min at –70 °C and then at –40 °C for 2 h. Subsequently, the reaction was left to proceed in the dark at room temperature (RT) overnight. Complete conversion of the starting aldehyde was verified by TLC (EtOAc/hexane 20:80). Then, an equal volume of saturated NH₄Cl_(aq) was added to the reaction mixture and the organic layer was extracted with Et₂O (for ferrocenyl retinoids) or EtOAc (for phenanthryl and *N*-alkylcarbazolyl retinoids). The combined organic extracts were washed with H₂O, dried over Na₂SO₄, and the solvent was evaporated in vacuo. The residue was purified by CC.

DIBAL-H reductions: To a stirred solution of the corresponding ester (2.6 mmol) in dry THF (18 mL) was added dropwise DIBAL-H (7.8 mmol, 1.2 M in hexane) at –70 °C under argon atmosphere. The mixture was treated with 6 N HCl until the suspension dissolved (at pH 1–2), and the organic layer was extracted with EtOAc. The extracts were washed with H₂O, dried over Na₂SO₄, and the solvent was evaporated in vacuo.

MnO₂ oxidations: To a stirred solution of the corresponding alcohol (2.6 mmol) in dry CH₂Cl₂ (25 mL) was added a fivefold excess (*w/w* relative to the alcohol) of dried MnO₂.^[31] The suspension was stirred at RT until the reaction was completed for 2 h (**1–4**), 4 h (**5**), 7 h (**6**) (monitored by TLC). The reaction mixture was filtered through Celite, the solids were washed with EtOAc, and the solvent from the organic layer was evaporated in vacuo. The residue was filtered through a short silica gel layer (eluent EtOAc/hexane 50:50) to remove residual MnO₂ and was employed directly in a subsequent HWE reaction.

Ester hydrolysis: Pure all-*trans* isomer of the corresponding ester (0.7 mmol, isomeric purity determined by ¹H NMR), obtained after HWE olefination, was suspended in MeOH (110 mL) and 5 N NaOH (55 mL). The mixture was held at reflux for 2 h (**1**, **14**), 4 h (**2–9**), 7 h (**10–12**), or 14 h (**13**). Complete hydrolysis of the ester was verified by TLC (20:80 EtOAc/hexane; 10% MeOH in CH₂Cl₂). The reaction mixture was then cooled to RT, neutralized to pH 7 with 6 N HCl, and subsequently an equal volume of H₂O was added. The organic layer was extracted with EtOAc and the extracts were washed with H₂O. Note that the organic layers should not be dried over Na₂SO₄ because of considerable irreversible sorption of the desired acid. The solvents were evaporated and the residue was dried in vacuo. The resulting oil was crystallized from hexane or 5–10% EtOAc in hexane to obtain the desired acid.

Synthesis of *N*-alkylcarbazoles:^[32] Powdered KOH (0.53 g, 9.5 mmol) was dissolved in DMSO (10 mL) at RT. A solution of carbazole (1.05 g, 6.3 mmol) in DMSO (6 mL) was added dropwise (H₂O bath cooling) and the corresponding alkyl iodide (9.5 mmol)

was added. The reaction mixture was stirred for 30 min, poured in H₂O (10 mL)/ice, and extracted with CH₂Cl₂. The combined organic extracts were washed with H₂O and brine, dried over Na₂SO₄, and the solvents were evaporated in vacuo. The residue was purified by CC on silica gel (1–5% EtOAc in hexane).

Synthesis of *N*-alkylcarbazol-3-aldehydes by Vilsmeier–Haack formylation.^[33]

To a stirred solution of the corresponding *N*-alkylcarbazole (5.8 mmol) in anhydrous DMF (10 mL) was added dropwise POCl₃ (40.6 mmol) under argon atmosphere and cooling (ice/H₂O). Subsequently, the reaction mixture was allowed to warm to RT for 1 h. It was then carefully heated and held at reflux (80 °C) for an additional 5 h. After that, the solution was poured on ice/H₂O and extracted with CH₂Cl₂. The combined extracts were washed with H₂O, dried over Na₂SO₄, and the solvents were evaporated in vacuo. The residue was purified by CC on silica gel (15% EtOAc in hexane).

Ethyl (all-*E*)-3-[*p*-(2'-ferrocenylethen-1'-yl)phenyl]prop-2-enoate:

Red oil (96% yield, Scheme 1 step d): ¹H NMR (400 MHz, CDCl₃): δ = 1.34 (t, *J* = 7.1 Hz, 3H, CH₃-ester), 4.15 (s, 5H, H-Fc), 4.27 (q, *J* = 7.1 Hz, 2H, CH₂-ester), 4.32 (s, 2H, H-Fc), 4.49 (s, 2H, H-Fc), 6.42 (d, *J* = 16.1 Hz, 1H, CH=), 6.68 (d, *J* = 16.1 Hz, 1H, CH=), 6.95 (d, *J* = 16.1 Hz, 1H, CH=), 7.43 (d, *J* = 8.3 Hz, 2H, Har), 7.49 (d, *J* = 8.3 Hz, 2H, Har), 7.67 ppm (d, *J* = 16.1 Hz, 1H, CH=); IR (film): $\tilde{\nu}$ = 3089 (m), 3027 (m), 2958 (m), 2925 (m), 2854 (m), 1708 (CO, s), 1630 (C=C, s), 1597 (s), 1313 (m), 1264 (m), 1206 (m), 1172 (s), 1039 (m), 814 cm⁻¹ (m); MS (EI, 70 eV) *m/z* (%): 386 (100) [*M*]⁺; HRMS: *m/z* [*M*]⁺ calcd for C₂₃H₂₂FeO₂: 386.0969, found: 386.0952.

(all-*E*)-3-[*p*-(2'-ferrocenylethen-1'-yl)phenyl]prop-2-enoic acid (1):

Red solid (24% total yield, Scheme 1 steps a,b,c,d,f): mp: > 290 °C (10% EtOAc/hexane); ¹H NMR (400 MHz, CDCl₃): δ = 4.15 (s, 5H, H-Fc), 4.33 (s, 2H, H-Fc), 4.49 (s, 2H, H-Fc), 6.44 (d, *J* = 16.0 Hz, 1H, CH=), 6.69 (d, *J* = 16.0 Hz, 1H, CH=), 6.97 (d, *J* = 16.0 Hz, 1H, CH=), 7.45 (d, *J* = 8.3 Hz, 2H, Har), 7.51 (d, *J* = 8.3 Hz, 2H, Har), 7.75 ppm (d, *J* = 16.0 Hz, 1H, CH=); IR (film): $\tilde{\nu}$ = 2500–3000 (br, O–H + C–H), 1677 (CO, s), 1623 (C=C, s), 1594 (s), 1426 (m), 1325 (m), 1223 (m), 1176 (m), 955 cm⁻¹ (m); MS (EI, 70 eV) *m/z* (%): 358 (100) [*M*]⁺; HRMS: *m/z* [*M*]⁺ calcd for C₂₁H₁₈FeO₂: 358.0656, found: 358.0654.

Methyl (1*E*,3*E*)-*p*-(4-ferrocenylbuta-1,3-dien-1-yl)benzoate:

Red solid (68% yield, Scheme 1 step a): mp: 188–189 °C (dec., 5% EtOAc in hexane); ¹H NMR (400 MHz, CDCl₃): δ = 3.91 (s, 3H, COOCH₃), 4.14 (s, 5H, H-Fc), 4.31 (s, 2H, H-Fc), 4.43 (s, 2H, H-Fc), 6.45–6.65 (m, 3H, CH=), 6.94 (dd, *J* = 15.6 Hz, *J* = 9 Hz, 1H, CH=), 7.45 (d, *J* = 8.4 Hz, 2H, Har), 7.98 ppm (d, *J* = 8.4 Hz, 2H, Har); ¹³C NMR (100 MHz, CDCl₃): δ = 52.0 (q), 67.1 (d, 2×), 69.4 (d, 7×), 82.6 (s), 125.8 (d, 2×), 126.5 (d), 128.2 (s), 128.6 (d), 130.0 (d, 2×), 132.3 (d), 133.7 (d), 142.4 (s), 167.0 ppm (s, COOH); IR (film): $\tilde{\nu}$ = 3095 (m), 2946 (m), 1711 (CO, s), 1598 (C=C, m), 1280 (s), 1107 (m), 993 cm⁻¹ (m); MS (EI, 70 eV) *m/z* (%): 372 (100) [*M*]⁺, 191 (17), 170 (16); HRMS: *m/z* [*M*]⁺ calcd for C₂₂H₂₀FeO₂: 372.0813, found: 372.0811.

(1*E*,3*E*)-*p*-(4-ferrocenylbuta-1,3-dien-1-yl)benzoic acid 2:

Red solid (54% total yield, Scheme 1 steps d,b,c,a,f): mp: > 290 °C (10% EtOAc in hexane); ¹H NMR (400 MHz, [D₆]DMSO): δ = 4.14 (s, 5H, H-Fc), 4.35 (s, 2H, H-Fc), 4.54 (s, 2H, H-Fc), 6.59 (d, *J* = 15.4 Hz, 1H, CH=), 6.64 (dd, *J* = 15.4 Hz, *J* = 9.0 Hz, 1H, CH=), 6.68 (d, *J* = 15.4 Hz, 1H, CH=), 7.12 (dd, *J* = 15.4 Hz, *J* = 9.0 Hz, 1H, CH=), 7.57 (d, *J* = 8.3 Hz, 2H, Har), 7.88 ppm (d, *J* = 8.3 Hz, 2H, Har); ¹³C NMR (100 MHz, [D₆]DMSO): δ = 66.8 (d, 2×), 69.0 (d, 5×), 69.1 (d, 2×), 82.4 (s), 125.7 (d, 2×), 126.4 (d), 128.2 (d), 128.7 (s), 129.6 (d, 2×), 132.3 (d), 133.7 (d), 141.8 (s), 166.9 ppm (s, COOH); IR (film): $\tilde{\nu}$ = 2500–3250 (br, O–H + C–H), 1675 (CO, s), 1593 (C=C, s), 1418 (s),

1280 (s), 1179 (m), 984 (s), 937 (m), 807 (m), 766 cm⁻¹ (m); MS (EI, 70 eV) *m/z* (%): 358 (100) [*M*]⁺; 191 (27); HRMS: *m/z* calcd for C₂₁H₁₈FeO₂: 358.0656, found: 358.0653.

(all-*E*)-3,7-dimethyl-9-ferrocenylnona-2,4,6,8-tetraenoic acid 3.^[34]

Red oil (67% total yield, Scheme 1 steps e,b,c,e,f): ¹H NMR (400 MHz, CDCl₃): δ = 2.02 (s, 3H, CH₃), 2.37 (s, 3H, CH₃), 4.13 (s, 5H, H-Fc), 4.32 (s, 2H, H-Fc), 4.45 (s, 2H, H-Fc), 5.81 (s, 1H, H-2), 6.19 (d, *J* = 11.0 Hz, 1H, H-6), 6.32 (d, *J* = 14.5 Hz, 1H, H-4), 6.46 (s, 2H, H-8 + H-9), 6.90–7.10 ppm (m, 1H, H-5); IR (film): $\tilde{\nu}$ = 2750–3250 (br, OH), 2923 (m), 1673 (CO, s), 1603 (C=C, m), 1572 (s), 1254 (s), 1186 (s), 1153 (m), 956 cm⁻¹ (m); MS (EI, 70 eV) *m/z* (%): 362 (100) [*M*]⁺, 318 (25), 256 (46), 186 (25), 121 (17); HRMS: *m/z* [*M*]⁺ calcd for C₂₁H₂₂FeO₂: 362.0969, found: 362.0967.

Ethyl (all-*E*)-5-[*p*-(2'-ferrocenylethen-1'-yl)phenyl]-3-methylpenta-2,4-dienoate:

Red oil (82% yield, Scheme 1 step e): ¹H NMR (400 MHz, CDCl₃): δ = 1.31 (t, *J* = 7.1 Hz, 3H, CH₃-ester), 2.41 (s, 3H, CH₃), 4.16 (s, 5H, H-Fc), 4.20 (q, *J* = 7.1 Hz, 2H, CH₂-ester), 4.32 (s, 2H, H-Fc), 4.49 (s, 2H, H-Fc), 5.91 (s, 1H, H-2), 6.67 (d, *J* = 16.1 Hz, 1H, CH=), 6.81 (d, *J* = 16.1 Hz, 1H, CH=), 6.91 (d, *J* = 16.1 Hz, 1H, CH=), 6.93 (d, *J* = 16.1 Hz, 1H, CH=), 7.41 (s, 2H, Har), 7.42 ppm (s, 2H, Har); IR (film): $\tilde{\nu}$ = 3096 (m), 3030 (m), 2958 (m), 2924 (m), 2853 (m), 1706 (CO, s), 1592 (C=C, s), 1239 (m), 1152 (s), 1044 (m), 963 (m), 814 cm⁻¹ (m); MS (EI, 70 eV) *m/z* (%): 426 (100) [*M*]⁺; HRMS: *m/z* [*M*]⁺ calcd for C₂₆H₂₆FeO₂: 426.1282, found: 426.1262.

(all-*E*)-5-[*p*-(2'-ferrocenylethen-1'-yl)phenyl]-3-methylpenta-2,4-dienoic acid 4:

Red solid (25% total yield, Scheme 1 steps a,b,c,e,f): mp: > 290 °C (10% EtOAc/hexane); ¹H NMR (400 MHz, [D₆]DMSO): δ = 2.32 (s, 3H, CH₃), 4.15 (s, 5H, H-Fc), 4.34 (s, 2H, H-Fc), 4.57 (s, 2H, H-Fc), 5.96 (s, 1H, H-2), 6.77 (d, *J* = 15.8 Hz, 1H, CH=), 7.00 (d, *J* = 15.8 Hz, 1H, CH=), 7.04 (d, *J* = 15.8 Hz, 1H, CH=), 7.06 (d, *J* = 15.8 Hz, 1H, CH=), 7.49 (d, *J* = 8.2 Hz, 2H, Har), 7.56 ppm (d, *J* = 8.2 Hz, 2H, Har); IR (film): $\tilde{\nu}$ = 2750–3250 (br, O–H + C–H), 1667 (CO, s), 1587 (C=C, s), 1288 (s), 1250 (s), 1173 (s), 957 (s), 806 cm⁻¹ (s); MS (EI, 70 eV) *m/z* (%): 398 (100) [*M*]⁺; HRMS: *m/z* [*M*]⁺ calcd for C₂₄H₂₂FeO₂: 398.0969, found: 398.0965.

Ethyl (all-*E*)-3-[*p*-(2'-(9'-phenanthryl)ethen-1'-yl)phenyl]prop-2-enoate:

Yellow solid (71% yield, Scheme 1 step d): mp: 159 °C; ¹H NMR (400 MHz, CDCl₃): δ = 1.36 (t, *J* = 7.1 Hz, 3H, CH₃), 4.29 (q, *J* = 7.1 Hz, 2H, CH₂), 6.47 (d, *J* = 16.0 Hz, 1H, CH=), 7.20 (d, *J* = 16.0 Hz, 1H, CH=), 7.50–8.00 (m, 12H, Har + 2CH=), 8.23 (d, *J* = 7.9 Hz, 1H, Har), 8.66 (d, *J* = 7.9 Hz, 1H, Har), 8.73 ppm (d, *J* = 7.9 Hz, 1H, Har); ¹³C NMR (100 MHz, CDCl₃): δ = 14.3 (q), 60.5 (t), 118.0 (d), 122.5 (d), 123.2 (d), 124.5 (d), 124.8 (d), 126.6 (d), 126.7 (d, 2×), 126.8 (d), 127.1 (d, 2×), 127.6 (d), 128.5 (d, 2×), 128.7 (s), 130.3 (s), 130.5 (s), 130.6 (s), 131.2 (d), 131.7 (s), 133.6 (s), 133.9 (s), 139.5 (s), 144.0 (d), 167.0 ppm (s); IR (film): $\tilde{\nu}$ = 3028 (m), 2980 (C–H, m), 1707 (CO, s), 1632 (C=C, s), 1600 (m), 1309 (m), 1262 (m), 1205 (m), 1175 (s), 1038 (m), 963 (m), 747 (m), 723 (m) cm⁻¹; MS (EI, 70 eV) *m/z* (%): 378 (100) [*M*]⁺, 349 (22), 303 (20); HRMS: *m/z* [*M*]⁺ calcd for C₂₇H₂₂O₂: 378.1620, found: 378.1621.

(all-*E*)-3-[*p*-(2'-(9'-phenanthryl)ethen-1'-yl)phenyl]prop-2-enoic acid 5:

Yellow solid (38% total yield, Scheme 1 steps a,b,c,d,f): mp: 259–265 °C (dec.); ¹H NMR (400 MHz, [D₆]DMSO): δ = 6.59 (d, *J* = 16.2 Hz, 1H, CH=), 7.42 (d, *J* = 16.2 Hz, 1H, CH=), 7.63 (d, *J* = 16.2 Hz, 1H, CH=), 7.65–7.80 (m, 6H, Har), 7.86 (d, *J* = 8.3 Hz, 2H, Har), 8.05 (dd, *J* = 8.2 Hz, *J* = 2 Hz, 1H, Har), 8.19 (d, *J* = 16.2 Hz, 1H, CH=), 8.22 (s, 1H, Har), 8.48 (dd, *J* = 8.2 Hz, *J* = 2.1 Hz, 1H, Har), 8.83 (d, *J* = 8.2 Hz, 1H, Har), 8.90 ppm (dd, *J* = 8.2 Hz, *J* = 2.1 Hz, 1H, Har); ¹³C NMR (100 MHz, [D₆]DMSO): δ = 118.9 (d), 122.7 (d), 123.3 (d), 123.9 (d), 124.6 (d), 126.7 (d), 126.8 (d), 126.9 (d), 126.9 (d), 127.0 (d), 127.3 (d, 2×), 128.6 (d, 3×), 129.6 (s), 129.9 (s), 130.0 (s),

131.0 (d), 131.2 (s), 132.9 (s), 133.6 (s), 139.0 (s), 143.4 (d), 167.6 ppm (s); IR (film): $\tilde{\nu}$ = 2500–3500 (br, O–H + C–H), 1678 (CO, s), 1623 (C=C, s), 1597 (s), 1422 (s), 1311 (s), 1282 (s), 1214 (s), 948 (s), 741 (s), 717 cm⁻¹ (s); MS (EI, 70 eV) m/z (%): 350 (100) [M]⁺, 303 (19), 202 (16); HRMS: m/z [M]⁺ calcd for C₂₅H₁₈O₂: 350.1307, found: 350.1305.

Methyl (1E,3E)-p-[4-(9'-phenanthryl)buta-1,3-dien-1-yl]benzoate: Orange solid (100% yield, Scheme 1 step a): mp: 179–180 °C; ¹H NMR (400 MHz, CDCl₃): δ = 3.93 (s, 3H, COOCH₃), 6.79 (d, J = 15.4 Hz, 1H, CH=), 7.13 (dd, J = 15.4 Hz, J = 10.3 Hz, 1H, CH=), 7.25 (dd, J = 15.4 Hz, J = 10.3 Hz, 1H, CH=), 7.50–7.80 (m, 7H, Har + CH=), 7.91 (dd, J = 7.8 Hz, J = 1.7 Hz, 1H, Har), 7.96 (s, 1H, Har), 8.03 (d, J = 8.3 Hz, 2H, Har), 8.24 (dd, J = 7.8 Hz, J = 1.7 Hz, 1H, Har), 8.67 (d, J = 7.8 Hz, 1H, Har), 8.75 ppm (d, J = 7.8 Hz, 1H, Har); ¹³C NMR (100 MHz, CDCl₃): δ = 52.0 (q), 122.5 (d), 123.2 (d), 124.3 (d), 124.5 (d), 126.2 (d, 2 \times), 126.6 (d), 126.7 (d, 2 \times), 126.9 (d), 128.7 (d), 128.9 (s), 130.0 (d, 2 \times), 130.3 (s), 130.4 (s), 130.5 (s), 131.6 (d), 131.7 (s), 131.9 (d, 2 \times), 131.9 (d), 133.2 (s), 141.8 (s), 166.9 ppm (s); IR (film): $\tilde{\nu}$ = 3028 (w), 2949 (C–H, w), 1713 (CO, s), 1600 (C=C, m), 1434 (m), 1413 (m), 1275 (s), 1175 (m), 1106 (m), 984 (m) cm⁻¹; MS (EI, 70 eV) m/z (%): 364 (100) [M]⁺, 305 (31), 215 (66), 69 (17); HRMS: m/z [M]⁺ calcd for C₂₆H₂₀O₂: 364.1463, found: 364.1463; Anal. calcd for C₂₆H₂₀O₂: C 85.69, H 5.53, found: C 85.63, H 5.59.

(1E,3E)-p-[4-(9'-phenanthryl)buta-1,3-dien-1-yl]benzoic acid 6: Orange solid (61% total yield, Scheme 1 steps d,b,c,a,f): mp: 262–266 °C; ¹H NMR (400 MHz, [D₆]DMSO): δ = 6.93 (d, J = 15.3 Hz, 1H, CH=), 7.31 (dd, J = 15.3 Hz, J = 10.5 Hz, 1H, CH=), 7.49 (dd, J = 15.3 Hz, J = 10.5 Hz, 1H, CH=), 7.60–7.80 (m, 7H, 6Har + CH=), 7.95 (d, J = 8.3 Hz, 2H, Har), 8.04 (dd, J = 7.2 Hz, J = 2.0 Hz, 1H, Har), 8.20 (s, 1H, Har), 8.30–8.40 (m, 1H, Har), 8.82 (dd, J = 7.2 Hz, J = 2.0 Hz, 1H, Har), 8.86–8.94 ppm (m, 1H, Har); ¹³C NMR (100 MHz, [D₆]DMSO): δ = 122.7 (d), 123.4 (d), 123.7 (d), 124.0 (d), 126.2 (d, 2 \times), 126.8 (d), 126.9 (d), 127.0 (d), 127.0 (d), 128.7 (d), 129.4 (s), 129.6 (s), 129.7 (s), 129.8 (d, 2 \times), 129.9 (s), 130.8 (d), 131.2 (s), 131.7 (d), 132.0 (d), 132.2 (d), 132.4 (s), 141.3 (s), 167.0 ppm (s); IR (film): $\tilde{\nu}$ = 2500–3250 (br, O–H + C–H), 1731 (w), 1682 (CO, s), 1595 (C=C, m), 1418 (m), 1285 (s), 970 (m), 756 (s) cm⁻¹; MS (EI, 70 eV) m/z (%): 350 (100) [M]⁺, 305 (22), 215 (68); HRMS: m/z [M]⁺ calcd for C₂₅H₁₈O₂: 350.1307, found: 350.1308.

Ethyl (all-E)-5-[p-[2'-(9'-phenanthryl)ethen-1'-yl]phenyl]-3-methylpenta-2,4-dienoate: Yellow solid (75% yield, Scheme 1 step e): mp: 146 °C; ¹H NMR (400 MHz, CDCl₃): δ = 1.32 (t, J = 7.1 Hz, 3H, CH₃ ester), 2.44 (d, J = 0.9 Hz, 3H, CH₃), 4.22 (q, J = 7.1 Hz, 2H, CH₂ ester), 5.94 (s, 1H, H-2), 6.86 (d, J = 16.0 Hz, 1H, CH=), 6.97 (d, J = 16.0 Hz, 1H, CH=), 7.23 (d, J = 16.0 Hz, 1H, CH=), 7.52 (d, J = 8.3 Hz, 2H, Har), 7.55–7.75 (m, 6H, Har), 7.85–7.95 (m, 2H, Har + CH=), 7.98 (s, 1H, Har), 8.26 (dd, J = 8.0 Hz, J = 1.6 Hz, 1H, Har), 8.68 (d, J = 8.0 Hz, 1H, Har), 8.75 ppm (dd, J = 8.0 Hz, J = 1.6 Hz, 1H, Har); ¹³C NMR (100 MHz, CDCl₃): δ = 13.8 (q), 14.4 (q), 59.8 (t), 120.0 (d), 122.5 (d), 123.2 (d), 124.5 (d), 124.6 (d), 126.6 (d), 126.6 (d), 126.7 (d), 126.7 (d), 126.8 (d), 127.1 (d, 2 \times), 127.5 (d, 2 \times), 128.7 (d), 130.3 (s), 130.5 (s), 130.7 (s), 131.4 (d), 131.8 (s), 131.9 (d), 133.6 (d), 133.8 (s), 135.9 (s), 137.9 (s), 152.0 (s), 167.0 ppm (s); IR (film): $\tilde{\nu}$ = 3028 (w), 2980 (w), 1704 (CO, s), 1597 (C=C, m), 1238 (m), 1152 (s), 959 cm⁻¹ (m); MS (EI, 70 eV) m/z (%): 418 (100) [M]⁺, 345 (17), 203 (44); HRMS: m/z [M]⁺ calcd for C₃₀H₂₆O₂: 418.1933, found: 418.1925.

(all-E)-5-[p-[2'-(9'-phenanthryl)ethen-1'-yl]phenyl]-3-methylpenta-2,4-dienoic acid 7: Yellow solid (40% total yield, Scheme 1 steps a,b,c,e,f): mp: 226–228 °C; ¹H NMR (400 MHz, [D₆]DMSO): δ = 2.35 (s, 3H, CH₃), 6.00 (s, 1H, H-2), 7.07 (d, J = 16.1 Hz, 1H, CH=),

7.14 (d, J = 16.1 Hz, 1H, CH=), 7.40 (d, J = 16.1 Hz, 1H, CH=), 7.60–7.80 (m, 6H, Har), 7.82 (d, J = 8.3 Hz, 2H, Har), 8.05 (dd, J = 6.9 Hz, J = 2.1 Hz, 1H, Har), 8.15 (d, J = 16.1 Hz, 1H, CH=), 8.21 (s, 1H, Har), 8.48 (dd, J = 7.3 Hz, J = 1.8 Hz, 1H, Har), 8.83 (dd, J = 7.3 Hz, J = 1.8 Hz, 1H, Har), 8.90 ppm (dd, J = 7.3 Hz, J = 1.8 Hz, 1H, Har); ¹³C NMR (100 MHz, [D₆]DMSO): δ = 13.2 (q), 120.6 (d), 122.7 (d), 123.3 (d), 123.8 (d), 124.6 (d), 125.8 (d), 126.8 (d, 2 \times), 126.9 (d), 127.0 (d), 127.3 (d, 2 \times), 127.4 (d, 2 \times), 128.6 (d), 129.6 (s), 129.9 (s), 130.0 (s), 131.3 (s + d), 131.8 (d), 133.1 (s), 133.3 (d), 135.7 (s), 137.4 (s), 151.2 (s), 167.8 ppm (s); IR (film): $\tilde{\nu}$ = 2500–3500 (br, O–H + C–H), 1692 (CO, s), 1588 (C=C, s), 1415 (s), 1259 (s), 1173 (s), 957 (s), 852 (s), 740 (s), 719 cm⁻¹ (s); MS (EI, 70 eV) m/z (%): 390 (100) [M]⁺, 203 (34); HRMS: m/z [M]⁺ calcd for C₂₈H₂₂O₂: 390.1620, found: 390.1624; Anal. calcd for C₂₈H₂₂O₂: C 86.13, H 5.68, found: C 85.98, H 5.68.

Ethyl (2E,4E)-5-(N-ethylcarbazol-3'-yl)-3-methylpenta-2,4-dienoate: Yellow oil (90% yield, Scheme 1 step e): ¹H NMR (400 MHz, CDCl₃): δ = 1.31 (t, J = 7.2 Hz, 3H, CH₃), 1.42 (t, J = 7.2 Hz, 3H, CH₃), 2.46 (s, 3H, 3-CH₃), 4.20 (q, J = 7.2 Hz, 2H, CH₂), 4.34 (q, J = 7.2 Hz, 2H, CH₂), 5.91 (s, 1H, H-2), 6.86 (d, J = 16.0 Hz, 1H, CH=), 7.14 (d, J = 16.0 Hz, 1H, CH=), 7.24 (t, J = 7.9 Hz, 1H, Har), 7.35 (d, J = 7.9 Hz, 1H, Har), 7.39 (d, J = 7.9 Hz, 1H, Har), 7.47 (t, J = 7.9 Hz, 1H, Har), 7.60 (d, J = 7.9 Hz, 1H, Har), 8.09 (d, J = 7.9 Hz, 1H, Har), 8.17 ppm (s, 1H, Har); IR (film): $\tilde{\nu}$ = 3046 (m), 2978 (m), 2934 (m), 2898 (m), 1703 (CO, s), 1594 (C=C, s), 1473 (m), 1384 (m), 1347 (m), 1235 (s), 1150 (s), 960 (m), 748 (m) cm⁻¹; MS (EI, 70 eV) m/z (%): 333 (44) [M]⁺, 260 (100), 245 (16), 230 (16), 205 (26); HRMS: m/z [M]⁺ calcd for C₂₂H₂₃NO₂: 333.1729, found: 333.1728.

(2E,4E)-5-(N-ethylcarbazol-3'-yl)-3-methylpenta-2,4-dienoic acid 8: Yellow solid (81% total yield, Scheme 1 steps e,f): mp: 198–199 °C; ¹H NMR (400 MHz, [D₆]DMSO): δ = 1.32 (t, J = 7.1 Hz, 3H, CH₃), 2.38 (s, 3H, 3-CH₃), 4.45 (q, J = 7.1 Hz, 2H, CH₂), 5.94 (s, 1H, H-2), 7.09 (d, J = 16.2 Hz, 1H, CH=), 7.15–7.30 (m, 2H, Har + CH=), 7.47 (t, J = 8.1 Hz, 1H, Har), 7.61 (d, J = 8.1 Hz, 2H, Har), 7.74 (dd, J = 8.1 Hz, J = 1.4 Hz, 1H, Har), 8.16 (d, J = 8.1 Hz, 1H, Har), 8.41 ppm (s, 1H, Har); ¹³C NMR (100 MHz, [D₆]DMSO): δ = 13.3 (q), 13.6 (q), 37.0 (t), 109.3 (d), 109.3 (d), 118.9 (d), 119.1 (d), 119.5 (d), 120.4 (d), 122.1 (s), 122.5 (s), 125.1 (d), 126.0 (d), 127.2 (s), 128.9 (d), 135.0 (d), 139.7 (s), 139.9 (s), 151.9 (s), 167.9 ppm (s); IR (film): $\tilde{\nu}$ = 2250–3250 (br, O–H + C–H), 1675 (CO, m), 1570 (C=C, s), 1340 (m), 1281 (m), 1252 (m), 1228 (m), 1171 (s), 922 cm⁻¹ (m), 720 (s); MS (EI, 70 eV) m/z (%): 305 (45) [M]⁺, 260 (100), 245 (24), 230 (28); HRMS: m/z [M]⁺ calcd for C₂₀H₁₉NO₂: 305.1416, found: 305.1416; Anal. calcd for C₂₀H₁₉NO₂: C 78.66, H 6.27, N 4.59, found: C 78.62, H 6.33, N 4.40.

Methyl (E)-p-[2-(N-ethylcarbazol-3'-yl)ethen-1-yl]benzoate: Yellow solid (100% yield, Scheme 1 step a): mp: 123 °C; ¹H NMR (400 MHz, CDCl₃): δ = 1.46 (t, J = 7.2 Hz, 3H, CH₃), 3.93 (s, 3H, COOCH₃), 4.38 (q, J = 7.2 Hz, 2H, CH₂), 7.17 (d, J = 15.4 Hz, 1H, CH=), 7.26 (d, J = 15.4 Hz, 1H, CH=), 7.35–7.55 (m, 4H, Har), 7.61 (d, J = 8.3 Hz, 2H, Har), 7.70 (dd, J = 8.3 Hz, J = 1.2 Hz, 1H, Har), 8.04 (d, J = 8.3 Hz, 2H, Har), 8.14 (d, J = 8.3 Hz, 1H, Har), 8.26 ppm (s, 1H, Har); ¹³C NMR (100 MHz, CDCl₃): δ = 13.8 (q), 37.7 (t), 52.0 (q), 108.7 (d), 108.7 (d), 119.2 (d), 119.2 (d), 120.5 (d), 122.9 (s), 123.4 (s), 124.6 (d), 124.8 (d), 125.9 (d, 2 \times), 126.0 (d), 127.9 (s), 128.2 (s), 130.0 (d, 2 \times), 132.3 (d), 140.1 (s), 140.4 (s), 142.6 (s), 167.0 ppm (s); IR (film): $\tilde{\nu}$ = 3022 (w), 2976 (w), 2949 (w), 2889 (w), 1713 (CO, s), 1596 (C=C, s), 1473 (m), 1280 (s), 1233 (m), 1178 (m), 1107 (m), 960 (m), 747 cm⁻¹ (m); MS (EI, 70 eV) m/z (%): 355 (100) [M]⁺, 154 (14); HRMS: m/z [M]⁺ calcd for C₂₄H₂₁NO₂: 355.1572, found: 355.1583; Anal. calcd for C₂₄H₂₁NO₂: C 81.10, H 5.96, N 3.94, found: C 81.33, H 6.00, N 3.87.

(E)-p-[2-(N-ethylcarbazol-3'-yl)ethen-1-yl]benzoic acid 9. Yellow solid (94% total yield, Scheme 1 steps a,f): mp: 274–277 °C; ¹H NMR (400 MHz, [D₆]DMSO): δ = 1.33 (t, *J* = 7.1 Hz, 3H, CH₃), 4.46 (q, *J* = 7.1 Hz, 2H, CH₂), 7.24 (t, *J* = 7.3 Hz, 1H, Har), 7.35 (d, *J* = 16.4 Hz, 1H, CH=), 7.48 (t, *J* = 7.3 Hz, 1H, Har), 7.59 (d, *J* = 16.4 Hz, 1H, CH=), 7.62 (d, *J* = 8.2 Hz, 1H, Har), 7.64 (d, *J* = 8.2 Hz, 1H, Har), 7.73 (d, *J* = 8.3 Hz, 2H, Har), 7.79 (dd, *J* = 8.1 Hz, *J* = 1.3 Hz, 1H, Har), 7.95 (d, *J* = 8.3 Hz, 2H, Har), 8.19 (d, *J* = 8.1 Hz, 1H, Har), 8.45 ppm (s, 1H, Har); ¹³C NMR (100 MHz, [D₆]DMSO): δ = 13.7 (q), 37.0 (t), 109.3 (d), 109.3 (d), 119.0 (d, 2×), 120.4 (d), 122.1 (s), 122.5 (s), 124.4 (d), 124.9 (d), 125.9 (d, 3×), 127.7 (s), 128.7 (s), 129.7 (d, 2×), 132.0 (d), 139.5 (s), 139.9 (s), 142.1 (s), 167.1 ppm (s); IR (film): $\tilde{\nu}$ = 2250–3250 (br, O–H + C–H), 1679 (CO, s), 1595 (C=C, s), 1473 (m), 1424 (m), 1294 (s), 1231 (s), 1178 (s), 961 (m), 864 (m), 799 (m), 741 cm⁻¹ (s); MS (EI, 70 eV) *m/z* (%): 341 (100) [M]⁺, 326 (64), 97 (26), 83 (31), 69 (40); HRMS: *m/z* [M]⁺ calcd for C₂₃H₁₉NO₂: 341.1416, found: 341.1409.

Methyl (E)-p-[2-(N-propylcarbazol-3'-yl)ethen-1-yl]benzoate: Yellow solid (74% yield, Scheme 1 step a): mp: 144–145 °C; ¹H NMR (400 MHz, CDCl₃): δ = 0.99 (t, *J* = 7.3 Hz, 3H, CH₃), 1.85–2.00 (m, 2H, CH₂), 3.93 (s, 3H, COOCH₃), 4.29 (t, *J* = 7.3 Hz, 2H, CH₂), 7.17 (d, *J* = 16.3 Hz, H, CH=), 7.22–7.30 (m, H, Har), 7.35–7.55 (m, 4H, 3Har + CH=), 7.60 (d, *J* = 8.2 Hz, 2H, Har), 7.69 (dd, *J* = 8.2 Hz, *J* = 2 Hz, H, Har), 8.04 (d, *J* = 8.2 Hz, 2H, Har), 8.13 (d, *J* = 8.2 Hz, H, Har), 8.26 ppm (s, H, H-4'); ¹³C NMR (100 MHz, CDCl₃): δ = 11.8 (q), 22.3 (t), 44.7 (t), 52.0 (q), 109.0 (d), 109.0 (d), 119.1 (d), 119.1 (d), 120.4 (d), 122.8 (s), 123.2 (s), 124.6 (d), 124.7 (d), 125.9 (d, 3×), 127.9 (s), 128.2 (s), 130.0 (d, 2×), 132.3 (d), 140.6 (s), 140.9 (s), 142.6 (s), 167.0 ppm (s); IR (film): $\tilde{\nu}$ = 3052 (m), 2959 (m), 2872 (m), 1703 (CO, s), 1589 (s), 1465 (s), 1331 (s), 1276 (s), 1221 (s), 1175 (s), 1103 (s), 963 (s), 742 cm⁻¹ (s); MS (EI, 70 eV) *m/z* (%): 369 (100) [M]⁺, 340 (61); HRMS: *m/z* [M]⁺ calcd for C₂₅H₂₃NO₂: 369.1729, found: 369.1720; Anal. calcd for C₂₅H₂₃NO₂: C 81.27, H 6.27, N 3.79, found: C 81.01, H 6.27, N 3.81.

(E)-p-[2-(N-propylcarbazol-3'-yl)ethen-1-yl]benzoic acid 10: Yellow solid (73% total yield, Scheme 1 steps a,f): mp: 263–4 °C; ¹H NMR (400 MHz, [D₆]DMSO): δ = 0.89 (t, *J* = 7.1 Hz, 3H, CH₃), 1.70–1.90 (m, 2H, CH₂), 4.38 (t, *J* = 7.1 Hz, 2H, CH₂), 7.23 (t, *J* = 7.5 Hz, H, Har), 7.35 (d, *J* = 16.4 Hz, H, CH=), 7.47 (t, *J* = 7.5 Hz, H, Har), 7.53–7.68 (m, 3H, 2Har + CH=), 7.72 (d, *J* = 8.2 Hz, 2H, Har), 7.78 (d, *J* = 8.2 Hz, H, Har), 7.95 (d, *J* = 8.2 Hz, 2H, Har), 8.18 (d, *J* = 8.2 Hz, H, Har), 8.44 ppm (s, H, H-4'); ¹³C NMR (100 MHz, [D₆]DMSO): δ = 11.3 (q), 21.8 (t), 43.7 (t), 109.5 (d), 109.6 (d), 118.9 (d), 118.9 (d), 120.3 (d), 122.0 (s), 122.3 (s), 124.4 (d), 124.8 (d), 125.9 (d, 3×), 127.6 (s), 128.7 (s), 129.7 (d, 2×), 132.0 (d), 140.1 (s), 140.5 (s), 142.0 (s), 167.1 ppm (s); IR (film): $\tilde{\nu}$ = 2250–3250 (br, O–H + C–H), 1674 (CO, s), 1593 (C=C, s), 1480 (m), 1422 (m), 1290 (s), 1223 (m), 1174 (m), 1141 (m), 943 (m), 738 cm⁻¹ (m); MS (EI, 70 eV) *m/z* (%): 355 (100) [M]⁺, 326 (95); HRMS: *m/z* [M]⁺ calcd for C₂₄H₂₁NO₂: 355.1572, found: 355.1558; Anal. calcd for C₂₄H₂₁NO₂: C 81.10, H 5.96, N 3.94, found: C 81.26, H 6.01, N 3.92.

Methyl (E)-p-[2-(N-butylcarbazol-3'-yl)ethen-1-yl]benzoate: Yellow solid (75% yield, Scheme 1 step a): mp: 127–128 °C; ¹H NMR (400 MHz, CDCl₃): δ = 0.96 (t, *J* = 7.2 Hz, 3H, CH₃), 1.35–1.50 (m, 2H, CH₂), 1.80–1.95 (m, 2H, CH₂), 3.93 (s, 3H, COOCH₃), 4.32 (t, *J* = 7.2 Hz, 2H, CH₂), 7.17 (d, *J* = 16.3 Hz, 1H, CH=), 7.22–7.30 (m, H, Har), 7.35–7.55 (m, 4H, 3Har + CH=), 7.60 (d, *J* = 8.1 Hz, 2H, Har), 7.69 (d, *J* = 8.1 Hz, H, Har), 8.04 (d, *J* = 8.1 Hz, 2H, Har), 8.13 (d, *J* = 8.1 Hz, H, Har), 8.25 ppm (s, H, H-4'); ¹³C NMR (100 MHz, CDCl₃): δ = 13.8 (q), 20.5 (t), 31.1 (t), 43.0 (t), 52.0 (q), 108.9 (d), 109.0 (d), 119.1 (d), 119.1 (d), 120.4 (d), 122.8 (s), 123.2 (s), 124.6 (d), 124.8 (d), 125.9 (d, 3×), 127.9 (s), 128.2 (s), 130.0 (d, 2×), 132.3 (d), 140.6 (s),

140.9 (s), 142.6 (s), 167.0 ppm (s); IR (film): $\tilde{\nu}$ = 3051 (m), 3022 (m), 2954 (m), 2926 (m), 2870 (m), 1710 (CO, s), 1591 (s), 1466 (m), 1335 (m), 1278 (s), 1176 (s), 1102 (s), 960 (s), 802 (s), 741 cm⁻¹ (s); MS (EI, 70 eV) *m/z* (%): 383 (100) [M]⁺, 340 (87), 280 (16), 154 (48); HRMS: *m/z* [M]⁺ calcd for C₂₆H₂₅NO₂: 383.1885, found: 383.1881; Anal. calcd for C₂₆H₂₅NO₂: C 81.43, H 6.57, N 3.65, found: C 81.46, H 6.55, N 3.62.

(E)-p-[2-(N-butylcarbazol-3'-yl)ethen-1-yl]benzoic acid 11: Yellow solid (75% total yield, Scheme 1 steps a,f): mp: 253 °C (dec.); ¹H NMR (400 MHz, [D₆]DMSO): δ = 0.89 (t, *J* = 7.1 Hz, 3H, CH₃), 1.25–1.40 (m, 2H, CH₂), 1.70–1.85 (m, 2H, CH₂), 4.41 (t, *J* = 7.1 Hz, 2H, CH₂), 7.23 (t, *J* = 7.5 Hz, H, Har), 7.35 (d, *J* = 16.6 Hz, H, CH=), 7.47 (t, *J* = 7.5 Hz, H, Har), 7.52–7.67 (m, 3H, 2Har + CH=), 7.72 (d, *J* = 8.2 Hz, 2H, Har), 7.78 (d, *J* = 8.2 Hz, H, Har), 7.95 (d, *J* = 8.2 Hz, 2H, Har), 8.18 (d, *J* = 8.2 Hz, H, Har), 8.44 ppm (s, H, H-4'); ¹³C NMR (100 MHz, [D₆]DMSO): δ = 13.6 (q), 19.67 (t), 30.6 (t), 42.0 (t), 109.4 (d), 109.5 (d), 118.9 (d), 118.9 (d), 120.3 (d), 122.0 (s), 122.4 (s), 124.4 (d), 124.9 (d), 125.9 (d, 3×), 127.6 (s), 128.7 (s), 129.7 (d, 2×), 132.0 (d), 140.0 (s), 140.4 (s), 142.0 (s), 167.1 ppm (s); IR (film): $\tilde{\nu}$ = 2400–3200 (br, O–H + C–H), 1676 (CO, s), 1590 (C=C, s), 1488 (m), 1420 (s), 1315 (s), 1289 (s), 1176 (s), 942 (s), 863 (m), 800 (s), 739 cm⁻¹ (s); MS (EI, 70 eV) *m/z* (%): 369 (86) [M]⁺, 326 (68), 148 (100), 83 (15), 69 (18); HRMS: *m/z* [M]⁺ calcd for C₂₅H₂₃NO₂: 369.1729, found: 369.1746; Anal. calcd for C₂₅H₂₃NO₂: C 81.27, H 6.27, N 3.79, found: C 81.01, H 6.45, N 3.64.

Methyl (E)-p-[2-(N-pentylcarbazol-3'-yl)ethen-1-yl]benzoate: Yellow solid (57% yield, Scheme 1 step a): mp: 104–105 °C; ¹H NMR (400 MHz, CDCl₃): δ = 1.85–1.95 (m, 3H, CH₃), 1.30–1.45 (m, 4H, CH₂-CH₂), 1.85–1.97 (m, 2H, CH₂), 3.93 (s, 3H, COOCH₃), 4.31 (t, *J* = 7.2 Hz, 2H, CH₂), 7.17 (d, *J* = 16.3 Hz, H, CH=), 7.22–7.30 (m, H, Har), 7.35–7.55 (m, 4H, 3Har + CH=), 7.61 (d, *J* = 8.2 Hz, 2H, Har), 7.69 (dd, *J* = 8.2 Hz, *J* = 1.7 Hz, H, Har), 8.04 (dd, *J* = 8.2 Hz, *J* = 1.7 Hz, 2H, Har), 8.13 (d, *J* = 8.2 Hz, H, Har), 8.26 ppm (s, H, H-4'); ¹³C NMR (100 MHz, CDCl₃): δ = 13.9 (q), 22.4 (t), 28.7 (t), 29.4 (t), 43.2 (t), 52.0 (q), 108.9 (d), 109.0 (d), 119.1 (d), 120.4 (d), 122.8 (s), 123.2 (s), 124.6 (d), 124.7 (d), 124.8 (d), 125.9 (d, 2×), 127.9 (s), 128.2 (s), 130.0 (d, 2×), 132.2 (d), 132.3 (d), 140.6 (s), 140.9 (s), 142.6 (s), 167.0 ppm (s); IR (film): $\tilde{\nu}$ = 3023 (m), 2950 (m), 2929 (m), 2865 (w), 1716 (CO, s), 1593 (s), 1469 (m), 1276 (s), 1175 (s), 1102 (s), 945 (m), 795 (m), 738 cm⁻¹ (s); MS (EI, 70 eV) *m/z* (%): 397 (100) [M]⁺, 340 (59); HRMS: *m/z* [M]⁺ calcd for C₂₇H₂₇NO₂: 397.5088, found: 397.2051; Anal. calcd for C₂₇H₂₇NO₂: C 81.58, H 6.85, N 3.52, found: C 81.44, H 6.91, N 3.50.

(E)-p-[2-(N-pentylcarbazol-3'-yl)ethen-1-yl]benzoic acid 12: Yellow solid (57% total yield, Scheme 1 steps a,f): mp: 226–227 °C (dec.); ¹H NMR (400 MHz, [D₆]DMSO): δ = 0.82 (t, 3H, *J* = 6.8 Hz, CH₃), 1.20–1.40 (m, 4H, 2CH₂), 1.70–1.85 (m, 2H, CH₂), 4.40 (t, *J* = 6.8 Hz, 2H, CH₂), 7.23 (t, *J* = 7.5 Hz, H, Har), 7.35 (d, *J* = 16.4 Hz, H, CH=), 7.47 (t, *J* = 7.5 Hz, H, Har), 7.53–7.68 (m, 3H, 2Har + CH=), 7.72 (d, *J* = 8.2 Hz, 2H, Har), 7.78 (d, *J* = 8.2 Hz, H, Har), 7.94 (d, *J* = 8.2 Hz, 2H, Har), 8.18 (d, *J* = 8.2 Hz, H, Har), 8.44 ppm (s, H, H-4'); ¹³C NMR (100 MHz, [D₆]DMSO): δ = 13.8 (q), 21.8 (t), 28.2 (t), 28.5 (t), 42.2 (t), 109.4 (d), 109.5 (d), 118.9 (d, 2×), 120.3 (d), 122.0 (s), 122.4 (s), 124.4 (d), 124.9 (d), 125.9 (d, 3×), 127.6 (s), 128.7 (s), 129.7 (d, 2×), 132.0 (d), 140.0 (s), 140.4 (s), 142.0 (s), 167.1 ppm (s); IR (film): $\tilde{\nu}$ = 2350–3200 (br, O–H + C–H), 1675 (CO, s), 1592 (C=C, s), 1486 (m), 1420 (m), 1289 (s), 1225 (m), 1174 (m), 941 (m), 736 cm⁻¹ (s). MS (EI, 70 eV) *m/z* (%): 383 (100) [M]⁺, 355 (15), 326 (92); HRMS: *m/z* [M]⁺ calcd for C₂₆H₂₅NO₂: 383.1885, found: 383.1878; Anal. calcd for C₂₆H₂₅NO₂: C 81.43, H 6.57, N 3.65, found: C 81.28, H 6.60, N 3.63.

Methyl (E)-p-[2-(N-hexylcarbazol-3'-yl)ethen-1-yl]benzoate: Yellow solid (76% yield, Scheme 1 step a): mp: 98–99 °C; ¹H NMR (400 MHz, CDCl₃): δ = 0.87 (t, *J* = 7.0 Hz, 3H, CH₃), 1.20–1.47 (m, 6H, 3xCH₂), 1.80–1.95 (m, 2H, CH₂), 3.93 (s, 3H, COOCH₃), 4.31 (t, *J* = 7.0 Hz, 2H, CH₂), 7.17 (d, *J* = 16.2 Hz, H, CH=), 7.22–7.30 (m, H, Har), 7.35–7.55 (m, 4H, 3Har + CH=), 7.61 (d, *J* = 8.2 Hz, 2H, Har), 7.69 (d, *J* = 8.2 Hz, H, Har), 8.04 (d, *J* = 8.2 Hz, 2H, Har), 8.13 (d, *J* = 8.2 Hz, H, Har), 8.25 ppm (s, H, H-4'); ¹³C NMR (100 MHz, CDCl₃): δ = 14.0 (q), 22.5 (t), 26.9 (t), 29.0 (t), 31.6 (t), 43.2 (t), 52.0 (q), 108.9 (d), 109.0 (d), 119.1 (d, 2×), 120.4 (d), 122.8 (s), 123.3 (s), 124.6 (d), 124.8 (d), 125.9 (d, 3×), 127.9 (s), 128.2 (s), 130.0 (d, 2×), 132.3 (d), 140.6 (s), 140.9 (s), 142.6 (s), 167.0 ppm (s); IR (film): $\tilde{\nu}$ = 3045 (m), 2952 (m), 2921 (m), 2853 (w), 1709 (s), 1625 (w), 1594 (s), 1464 (m), 1277 (s), 1178 (s), 1105 (s), 954 (s), 797 (s), 742 (s), 690 (s), 607 cm⁻¹ (s); MS (EI, 70 eV) *m/z* (%): 411 (100) [M]⁺, 340 (58), 155 (16); HRMS: *m/z* [M]⁺ calcd for C₂₈H₂₉NO₂: 411.2198, found: 411.2195; Anal. calcd for C₂₈H₂₉NO₂: C 81.72, H 7.10, N 3.40, found: C 81.71, H 7.13, N 3.41.

(E)-p-[2-(N-hexylcarbazol-3'-yl)ethen-1-yl]benzoic acid 13: Yellow solid (76% total yield, Scheme 1 steps a,f): mp: 225–226 °C (dec.); ¹H NMR (400 MHz, [D₆]DMSO): δ = 0.81 (t, *J* = 6.9 Hz, 3H, CH₃), 1.10–1.40 (m, 6H, 3CH₂), 1.70–1.85 (m, 2H, CH₂), 4.40 (t, *J* = 6.9 Hz, 2H, CH₂), 7.23 (t, *J* = 7.5 Hz, H, Har), 7.35 (d, *J* = 16.4 Hz, H, CH=), 7.47 (t, *J* = 7.5 Hz, H, Har), 7.52–7.67 (m, 3H, 2Har + CH=), 7.72 (d, *J* = 8.2 Hz, 2H, Har), 7.78 (d, *J* = 8.2 Hz, H, Har), 7.94 (d, *J* = 8.2 Hz, 2H, Har), 8.18 (d, *J* = 8.2 Hz, H, Har), 8.44 ppm (s, H, H-4'); ¹³C NMR (100 MHz, [D₆]DMSO): δ = 13.7 (q), 21.9 (t), 26.0 (t), 28.4 (t), 30.8 (t), 42.2 (t), 109.4 (d), 109.5 (d), 118.9 (d, 2×), 120.3 (d), 122.0 (s), 122.3 (s), 124.4 (d), 124.8 (d), 125.9 (d, 3×), 127.6 (s), 128.7 (s), 129.7 (d, 2×), 132.0 (d), 140.0 (s), 140.4 (s), 142.0 (s), 167.1 ppm (s); IR (film): $\tilde{\nu}$ = 2300–3200 (br, O–H + C–H), 1674 (CO, s), 1590 (C=C, s), 1469 (s), 1416 (m), 1283 (s), 1178 (m), 957 (m), 930 (m), 868 (m), 795 (m), 736 cm⁻¹ (s); MS (EI, 70 eV) *m/z* (%): 397 (100) [M]⁺, 326 (73); HRMS: *m/z* [M]⁺ calcd for C₂₇H₂₇NO₂: 397.2042, found: 397.2036; Anal. calcd for C₂₇H₂₇NO₂: C 81.58, H 6.85, N 3.52, found: C 81.52, H 6.85, N 3.50.

(E)-p-(2-ferrocenyl-ethen-1-yl)benzoic acid 14: Red solid (50% total yield, Scheme 1 steps a,f): mp: >290 °C (10% EtOAc in hexane); ¹H NMR (400 MHz, [D₆]DMSO): δ = 4.15 (s, 5H, H-Fc), 4.36 (s, 2H, H-Fc), 4.60 (s, 2H, H-Fc), 6.83 (d, *J* = 16.5 Hz, 1H, CH=), 7.15 (d, *J* = 16.5 Hz, 1H, CH=), 7.59 (d, *J* = 8.2 Hz, 2H, Har), 7.89 ppm (d, *J* = 8.2 Hz, 2H, Har); ¹³C NMR (100 MHz, [D₆]DMSO): δ = 67.1 (d, 3×), 69.0 (d, 5×), 69.2 (d), 82.4 (s), 124.4 (d), 125.5 (d, 2×), 128.4 (s), 129.7 (d, 2×), 130.2 (d), 141.9 (s), 167.1 ppm (s, COOH); IR(film): $\tilde{\nu}$ = 3250–2750 (br, OH), 3089, 2981, 2672, 2548, 1676 (CO, s), 1596 (C=C, s), 1423 (s), 1288 (s), 1177 (m), 915 (s), 817 (s), 766 cm⁻¹ (s); MS (EI, 70 eV) *m/z* (%): 332 (100) [M]⁺, 165 (32); Anal. calcd for C₁₉H₁₆FeO₂: C 68.70, H 4.85, found: C 68.67, H 4.85.

Supporting Information contains characterization data for other intermediate compounds in the synthesis of ligands 1–14.

Biological assays

Materials and methods: Differentiation and apoptosis induction assays were performed on a FACScan flow cytometer (Becton Dickinson). Antibodies used for differentiation analyses were as follows (all from BD Pharmingen): PE anti-human CD11c or FITC anti-human CD14 in the test sample and PE mouse IgG₁ or FITC mouse IgG_{2a} antibodies, respectively, as isotypic control to determine the nonspecific background staining. Recombinant human Annexin V-FITC (Caltag Laboratories) was used as marker for apoptotic cells and PI (propidium iodide, Sigma–Aldrich) as a marker for necrotic

cells. Antibodies for caspases-8, -9, -10, cleaved caspase-3 and BID were purchased from Cell Signaling Technology, DR5 antibody was obtained from Sigma, DcR1 and DcR2 antibodies were from Chemicon International Inc., and TRAIL antibody was obtained from R&D Systems. All antibodies were used at 1:1000 dilution.

NB4 cells^[35] were purchased from the DSMZ, Germany. Cells were cultured in RPMI 1640 supplemented with 10% fetal calf serum (FCS), glutamine (2 mM), HEPES buffer (25 mM), and gentamycin (40 μg mL⁻¹), in a humidified incubator at 37 °C and 5% CO₂. Every two days the cells were diluted to 1 × 10⁵ cells mL⁻¹ and treated with the corresponding ligand (at 1 μM final concentration).

HeLa cells, stably transfected with (17m)₅-βG-Luc-Neo reporter^[26] and with Gal4-mRARα (or β, γ) or Gal4-hRXRβ plasmids, were maintained in DMEM with 5% FCS, geneticin (G418, 0.8 mg mL⁻¹), puromycin (0.3 μg mL⁻¹), and gentamycin (40 μg mL⁻¹); in case of the Gal4-hRXRβ HeLa cell line, hygromycin (0.2 mg mL⁻¹) was also added. The ligand binding assays were carried out in DMEM without red phenol with 5% charcoal-treated FCS. Luminescence was determined on a Berthold MicroLumat LB96P luminometer.

Western blot analysis: Cells (50 × 10⁵) were collected by centrifugation (500 *g*, 10 min), washed (PBS) and lysed in ice-cold buffer (10 mM Tris-HCl pH 7.5, 1 mM EDTA, 150 mM NaCl, 1% Nonidet P-40, 1 mM DTT) containing 1 × protease inhibitor cocktail (PIC tablets complete Roche Diagnostic GmbH, stock solution 25 × concentration), 0.1 mM phenylmethylsulfonyl fluoride (PMSF), and 100 μM Na₃VO₄. Cell lysates were clarified (12000 *g*, 15 min at 4 °C), and protein concentrations were determined by Quick Start™ Bradford Protein Assay Kit (Bio-Rad Laboratories, GmbH).

Cell lysates (60 μg protein per lane) were fractionated by sodium dodecyl sulfate polyacrylamide gel (12 or 15%) electrophoresis (SDS-PAGE) and then transferred on nitrocellulose membrane (Protran BA 85, 0.45 μm pore size, Whatman Schleicher & Schuell, GmbH). After that, the membranes were blocked with 5% nonfat dry milk in 1 × PBS for 1 h, incubated with primary antibody (overnight at 4 °C) and with secondary horseradish peroxidase (HRP)-linked antibody in 5% nonfat dry milk in 1 × PBS (1 h at RT). The membranes were washed (1% Tween in 1 × PBS), dried, and immunoreactive proteins were visualized using the Amersham Biosciences enhanced chemiluminescence (ECL) Western blotting detection system.

The following assays were performed as reported in Reference [36]: RAR/RXR transactivation analysis, differentiation induction assays, and apoptosis induction assays.

Acknowledgements

The work was supported by the European Commission ANTI-CANCER RETINOIDS, FP5 contract QLK3-CT-2002-02029. The Organizing Committee and Cold Spring Harbor Laboratory honored this work with a financial aid award at the "Nuclear Receptors: Bench to Bedside" International Conference, New York, USA (2006). The authors thank C. Gaudon, A. Bindler, and M. Lieb for excellent technical assistance.

Keywords: antitumor agents · apoptosis · drug discovery · receptors · structure–activity relationships

- [1] A. Melnick, J. D. Licht, *Blood* **1999**, *93*, 3167–3215.
- [2] The RAR α -PML but not the PML-RAR α transcript was detected in one APL patient: M. Lafage-Pochitaloff, M. Alcalay, V. Brunel, L. Longo, D. Sainty, J. Simonetti, F. Birg, P. G. Pelicci, *Blood* **1995**, *85*, 1169–1174.
- [3] L. He, M. Bhaumik, C. Tribioli, E. M. Rego, S. Ivins, A. Zelent, P. P. Pandolfi, *Mol. Cell* **2000**, *6*, 1131–1141.
- [4] D. R. Soprano, P. Qin, K. J. Soprano, *Annu. Rev. Nutr.* **2004**, *24*, 201–221.
- [5] W. Bourguet, P. Germain, H. Gronemeyer, *Trends Pharmacol. Sci.* **2000**, *21*, 381–388.
- [6] 9-*cis*-Retinoic acid is thought to be the putative natural pan-RAR/RXR ligand obtained in vivo by isomerization of its 'pro-hormone' ATRA.
- [7] PPAR: peroxisome proliferator-activated receptor, TR: thyroid hormone receptor, VDR: vitamin D receptor, LXR: liver X receptor.
- [8] Selective RXR modulators decreased glucose levels in mouse models of non-insulin-dependent diabetes mellitus without suppression of the thyroid hormone axis and without increase in blood triglycerides: P. Y. Michellys, R. J. Ardecky, J. H. Chen, D. L. Crombie, G. J. Etgen, M. M. Faul, A. L. Faulkner, T. A. Grese, R. A. Heyman, D. S. Karanewsky, K. Klausning, M. D. Leibowitz, S. Liu, D. A. Mais, C. M. Mapes, K. B. Marschke, A. Reifel-Miller, K. M. Ogilvie, D. Rungta, A. W. Thompson, J. S. Tyhonas, M. F. Boehm, *J. Med. Chem.* **2003**, *46*, 2683–2696.
- [9] D. Ivanova, H. Gronemeyer, A. R. de Lera, abstract at the international conference "Nuclear Receptors: Bench to Bedside", section: *Nuclear Receptors and Cancer*, Cold Spring Harbor Laboratory, New York (USA) **2006**, p. 30.
- [10] A. Konishi, E. Kawahara, M. Yoshikawa, T. Suzuki, M. Shimoda, M. Shoji, A. Kojima, Patent JP06059474 A2, **1994**, 0304.
- [11] R. G. Keedwell, Y. Zhao, L. A. Hammond, S. Qin, K.-Y. Tsang, A. Reitmair, Y. Molina, Y. Okawa, L. I. Atangan, D.-L. Shurland, K. Wen, D. Michael, A. Wallace, R. Bird, R. A. S. Chandraratna, G. Brown, *Cancer Res.* **2004**, *64*, 3302–3312.
- [12] J. A. Bandy, H. E. Bunting, M. L. H. Green, S. R. Marder, M. E. Thompson, D. Bloor, P. V. Kolinsky, R. J. Jones in *Organic Materials for Nonlinear Optics* (Eds.: R. A. Hann, D. Bloor), Royal Society of Chemistry, Special Publication No. 69, Burlington House, London, **1989**, pp. 219–224.
- [13] E. V. Mironova, A. Yu. Lukin, S. V. Shevyakov, S. G. Alexeeva, V. I. Shvets, O. V. Demina, A. A. Khodonov, L. V. Khitrina, *Biochemistry (Moscow)* **2001**, *66*, 1323–1333.
- [14] H. Mayer, W. Bollag, R. Hänni, R. Rügge, *Experientia* **1978**, *34*, 1105–1119.
- [15] a) M. Görmen, P. Pigeon, S. Top, E. A. Hillard, M. Huché, C. G. Hartinger, F. de Montigny, M. A. Plamont, A. Vessières, G. Joauen, *ChemMedChem* **2010**, *5*, 2039–2050; b) A. Nguyen, S. Top, P. Pigeon, A. Vessières, E. A. Hillard, M.-A. Plamont, M. Huché, C. Rigamonti, G. Joauen, *Chem. Eur. J.* **2009**, *15*, 684–696; c) S. Top, B. Dauer, J. Vaissermann, G. Joauen, *J. Organomet. Chem.* **1997**, *541*, 355–361.
- [16] S. R. S. Rudrangi, V. K. Bontha, S. Bethi, M. V. Reddy, *IJPRD (International Journal of Pharmaceutical Research and Development)* **2010**, *2*, 53–60.
- [17] D. Ivanova, C. Gaudon, A. Rossin, W. Bourget, H. Gronemeyer, *Bioorg. Med. Chem.* **2002**, *10*, 2099–2102.
- [18] A. le Maire, C. Teyssier, C. Erb, M. Grimaldi, S. Alvarez, A. R. de Lera, P. Balaguer, H. Gronemeyer, C. A. Royer, P. Germain, W. Bourguet, *Nat. Struct. Mol. Biol.* **2010**, *17*, 801–807.
- [19] P. Germain, S. Kammerer, E. Perez, C. Peluso-Iltis, D. Tortolani, F. C. Zusi, J. Starrett, P. Lapointe, J.-P. Daris, A. Marinier, A. R. de Lera, N. Rochel, H. Gronemeyer, *EMBO Rep.* **2004**, *5*, 877–882.
- [20] J.-P. Renaud, N. Rochel, M. Ruff, V. Vivat, P. Chambon, H. Gronemeyer, D. Moras, *Nature* **1995**, *378*, 681–689.
- [21] W. Bourguet, V. Vivat, J.-M. Wurtz, P. Chambon, H. Gronemeyer, D. Moras, *Mol. Cell* **2000**, *5*, 289–298.
- [22] G. Benbrook, M. M. Madler, L. W. Spruce, P. J. Birckbichler, E. C. Nelson, S. Subramanian, G. M. Weerasekare, J. B. Gale, M. K. Patterson Jr., B. Wang, W. Wang, S. Lu, T. C. Rowland, P. DiSivestro, C. Lindamood III, D. L. Hill, K. D. Berlin, *J. Med. Chem.* **1997**, *40*, 3567–3583.
- [23] G. V. Kryshstal, E. P. Serebryakov, *Izv. Akad. Nauk. Ser. Khim.* **1995**, *10*, 1867–1885; [*Russ. Chem. Bull.* **1995**, *44*, 1785–1804 (Engl. Transl.)].
- [24] Compound **3** (Ar=PHT), published in our previous work,^[17] activated RAR α and RAR β , but was discriminated by RAR γ (Met272) and RXR. It triggered differentiation of NB4 cells at a high percentage but with a low level of CD11c expression, and therefore apoptosis was not induced.
- [25] a) S. Green, P. Chambon, *Nature* **1987**, *325*, 75–78; b) R. M. Evans, *Mol. Endocrinol.* **2005**, *19*, 1429–1438; c) W. Bourguet, A. R. de Lera, H. Gronemeyer, *Meth. Enzymol.* **2010**, *485*, 161–195.
- [26] J.-Y. Chen, S. Penco, J. Ostrowski, P. Balaguer, M. Pons, J. E. Starrett, P. Reczek, P. Chambon, H. Gronemeyer, *EMBO J.* **1995**, *14*, 1187–1197.
- [27] a) H. Te Riele, E. R. Maandag, A. Clarke, M. Hooper, A. Berns, *Nature* **1990**, *348*, 649–651; b) S. Nagpal, S. Friant, H. Nakshatri, P. Chambon, *EMBO J.* **1993**, *12*, 2349–2360.
- [28] S. J. Martin, J. G. Bradley, T. G. Cotter, *Clin. Exp. Immunol.* **1990**, *79*, 448–453.
- [29] L. J. Donato, N. Noy, *Cancer Res.* **2005**, *65*, 8193–8199.
- [30] B. Domínguez, Y. Pazos, A. R. de Lera, *J. Org. Chem.* **2000**, *65*, 5917–5925.
- [31] MnO₂ was obtained by a standard procedure: a mixture of MnSO₄ (0.200 mol) and KMnO₄ (0.133 mol) in 600 mL H₂O was stirred for 1 h at RT, filtered, and washed until the filtrate remained colorless. The solid precipitate was then dried for two days at RT.
- [32] C. W. Brown, S. Liu, J. Klucik, K. D. Berlin, P. J. Brennan, D. Kaur, D. M. Benbrook, *J. Med. Chem.* **2004**, *47*, 1008–1017 (with modifications).
- [33] *Reactions and Syntheses in the Organic Chemistry Laboratory* (Eds.: L. F. Tietze, T. Eicher), University Science Books, Mill Valley, California, **1989**, Chapter 3.3, p. 330 (with modifications).
- [34] The ¹³C NMR spectrum of this ferrocene compound was not recorded because of ligand instability and rapid partial isomerization in solution.
- [35] a) M. J. S. Roussel, M. Lanotte, *Oncogene* **2001**, *20*, 7287–7291; b) G. Benoit, M. Roussel, F. Pendino, E. Ségal-Bendirdjian, M. Lanotte, *Oncogene* **2001**, *20*, 7161–7177.
- [36] M. W. Büttner, Ch. Burschka, J. O. Daiss, D. Ivanova, N. Rochel, S. Kammerer, C. Peluso-Iltis, A. Bindler, C. Gaudon, P. Germain, D. Moras, H. Gronemeyer, R. Tacke, *ChemBioChem* **2007**, *8*, 1688–1699.

Received: February 5, 2011

Revised: March 4, 2011

Published online on April 19, 2011

Please note: Minor changes to this article in *ChemMedChem* were made after publication in EarlyView. In particular, Prof. Angel R. de Lera was moved from the Acknowledgements to become a co-author of the paper. Also, the addition of a reference necessitated the removal of two sentences from the discussion. The scientific results and conclusions remain unaffected. The Editor.